ELEMENTA
Science of the Anthropocene

Simpson, IJ, et al. 2020. Characterization, sources and reactivity of volatile organic compounds (VOCs) in Seoul and surrounding regions during KORUS-AQ. *Elem Sci Anth,* 8: 37. DOI: https://doi.org/10.1525/elementa.434

RESEARCH ARTICLE

# Characterization, sources and reactivity of volatile organic compounds (VOCs) in Seoul and surrounding regions during KORUS-AQ

Isobel J. Simpson[*], Donald R. Blake[*], Nicola J. Blake[*], Simone Meinardi[*], Barbara Barletta[*], Stacey C. Hughes[*], Lauren T. Fleming[*,†], James H. Crawford[‡], Glenn S. Diskin[‡], Louisa K. Emmons[§], Alan Fried[‖], Hai Guo[¶], David A. Peterson[**], Armin Wisthaler[††,‡‡], Jung-Hun Woo[§§], Jerome Barré[§,‖‖], Benjamin Gaubert[§], Jinseok Kim[§§], Michelle J. Kim[¶¶], Younha Kim[§§,§§§], Christoph Knote[***], Tomas Mikoviny[††], Sally E. Pusede[†††], Jason R. Schroeder[‡,‡‡‡], Yu Wang[¶], Paul O. Wennberg[¶¶] and Lewei Zeng[¶]

The Korea-United States Air Quality Study (KORUS-AQ) took place in spring 2016 to better understand air pollution in Korea. In support of KORUS-AQ, 2554 whole air samples (WAS) were collected aboard the NASA DC-8 research aircraft and analyzed for 82 $C_1$–$C_{10}$ volatile organic compounds (VOCs) using multi-column gas chromatography. Together with fast-response measurements from other groups, the air samples were used to characterize the VOC composition in Seoul and surrounding regions, determine which VOCs are major ozone precursors in Seoul, and identify the sources of these reactive VOCs. (1) The WAS VOCs showed distinct signatures depending on their source origins. Air collected over Seoul had abundant ethane, propane, toluene and *n*-butane while plumes from the Daesan petrochemical complex were rich in ethene, $C_2$–$C_6$ alkanes and benzene. Carbonyl sulfide (COS), CFC-113, CFC-114, carbon tetrachloride ($CCl_4$) and 1,2-dichloroethane were good tracers of air originating from China. CFC-11 was also elevated in air from China but was surprisingly more elevated in air over Seoul. (2) Methanol, isoprene, toluene, xylenes and ethene were strong individual contributors to OH reactivity in Seoul. However methanol contributed less to ozone formation based on photochemical box modeling, which better accounts for radical chemistry. (3) Positive Matrix Factorization (PMF) and other techniques indicated a mix of VOC source influences in Seoul, including solvents, traffic, biogenic, and long-range transport. The solvent and traffic sources were roughly equal using PMF, and the solvents source was stronger in the KORUS-AQ emission inventory. Based on PMF, ethene and propene were primarily associated with traffic, and toluene, ethylbenzene and xylenes with solvents, especially non-paint solvents for toluene and paint solvents for ethylbenzene and xylenes. This suggests that VOC control strategies in Seoul could continue to target vehicle exhaust and paint solvents, with additional regulations to limit the VOC content in a variety of non-paint solvents.

**Keywords:** VOCs; Seoul; Korea; KORUS-AQ; Source apportionment; OH reactivity

## 1. Introduction

Air pollution is an environmental and human health concern throughout the world. As well as impacting respiratory and heart diseases, the International Agency for Research on Cancer (IARC) has classified outdoor air pollution as a carcinogen (*IARC*, 2013). Components of air pollution such as ozone ($O_3$) damage vegetation and are harmful to humans (*Ainsworth et al.*, 2012). While

* University of California, Irvine, CA, US
† University of Leeds, Leeds, UK
‡ NASA Langley, Hampton, VA, US
§ NCAR, Boulder, CO, US
‖ University of Colorado, Boulder, CO, US
¶ The Hong Kong Polytechnic University, Hong Kong, CN
** Naval Research Laboratory, Monterey, CA, US
†† University of Oslo, Oslo, NO
‡‡ University of Innsbruck, Innsbruck, AT
§§ Konkuk University, Seoul, KR
‖‖ European Centre for Medium-Range Weather Forecasts, Reading, UK
¶¶ California Institute of Technology, Pasadena, CA, US
*** Meteorological Institute, LMU Munich, Munich, DE
††† University of Virginia, Charlottesville, VA, US
‡‡‡ California Air Resources Board, Sacramento, CA, US
§§§ IIASA, Laxenburg, AT
Corresponding author: Isobel J. Simpson (isimpson@uci.edu)

emission controls on precursor gases such as volatile organic compounds (VOCs) and nitrogen oxides ($NO_x$) have led to decreases in $O_3$ levels and extreme $O_3$ events in North America and Europe, parts of Asia including South Korea have seen increasing long-term $O_3$ trends (*Chang et al.*, 2017; *Fleming et al.*, 2018). South Korea has an 8-hr $O_3$ standard of 60 ppbv, and the number of ozone exceedance days has increased from a low of 5 days in 2002 to 58 days in 2016 (*Seo et al.*, 2018).

In an effort to improve air quality, the Korean Ministry of Environment (KMOE) has ongoing policies to tighten environmental standards and reduce the emissions of major air pollutants (*KMOE*, 2017; *Shin et al.*, 2013). For example, multiple strategies have been used to target emissions from motor vehicles and gasoline evaporation in South Korea over the past two decades. Registered vehicles in South Korea are fueled primarily by gasoline (10.1 million vehicles), diesel (9.2 million) and liquefied petroleum gas (LPG; 2.2 million), with a smaller number fueled by compressed natural gas (CNG; ~39,000), electric (~11,000) and hybrid technology (~233,000) (*MOLIT*, 2016). Gasoline-fueled vehicles in South Korea have been subject to California's Non Methane Organic Gases Fleet Average System since 2009, and diesel-fueled vehicles have been regulated under Euro 6 emission standards since 2014. South Korea began a program to replace diesel-powered public buses with buses fueled by compressed natural gas (CNG) in 2000, and all transit buses in Seoul were fueled by CNG by 2010 (*ESCI*, 2013). To further improve air quality, about half the Seoul bus fleet will switch from CNG to electric during 2018–2025 (*Korea Herald*, 2018). VOCs have additional sources in South Korea such as organic solvents and production processes, and emission control strategies include the establishment of nation-wide VOC content limits for paints in 2013 (*KMOE*, 2017). While these emission control measures have led to an overall reduction in VOC levels in Seoul over the past twenty years, understanding the contributions of VOCs to ozone and aerosol formation in the Seoul Metropolitan Area (SMA) remains a high research priority (*Kim and Lee*, 2018).

In order to better understand the evolving factors that contribute to air pollution in the Korean peninsula, South Korea's National Institute of Environmental Research (NIER) and the United States National Aeronautics and Space Administration (NASA) led the Korea-United States Air Quality Study (KORUS-AQ), a cooperative field study that deployed in late spring 2016 (May 2 to June 10). The study included measurements of trace gases, aerosols and meteorological parameters from aircraft, ground-based stations and ships, together with modeling analysis of air quality and meteorology (*Crawford et al.*, 2020). South Korea has a temperate climate, with four distinct seasons that often exhibit large variations in meteorology. The mean wind direction is southwesterly in summer and northwesterly in winter (*KMA*, 2009). Dynamic mid-latitude meteorology facilitates transport of Asian dust to Korea in March and April, and the Asian monsoon wind shift brings heavy rains and occasional tropical disturbances to Korea, beginning in late June. The late spring measurement period of the KORUS-AQ mission was chosen to minimize long distance pollution transport and instead target local photochemical pollution. However, periods of dynamic transport were still encountered during the mission (*H. Kim et al.*, 2018a; *Peterson et al.*, 2019), which allowed inflow from other regions to be characterized. Designated flights over the West Sea, upwind of Korea, enabled sampling of Chinese emissions in isolation from Korea, even when these air masses were not expected to arrive in Korea. KORUS-AQ therefore offers a comprehensive suite of measurement data and modeling products from local and regional sources, influenced by variable springtime meteorology.

As part of KORUS-AQ, the University of California, Irvine (UCI) measured 82 speciated VOCs aboard the NASA DC-8 research aircraft using discrete whole air sampling (WAS) followed by multi-column gas chromatography. The measured VOCs include reactive gases such as toluene that can readily form secondary pollutants such as $O_3$ and secondary organic aerosol (SOA), and compounds that can have direct impacts on human health such as benzene. Limited ground-based measurements were also collected in Seoul in spring 2015 (the year before KORUS-AQ) using the same technique (*H. Kim et al.*, 2018; *S. Kim et al.*, 2016, 2018). High resolution instruments provided OVOC measurements during KORUS-AQ, including methanol and formaldehyde. Here we characterize VOC concentrations over Seoul, the Korean peninsula, and surrounding waters, including plumes from the Daesan petrochemical facility and in air originating from China. Additional comprehensive analysis of the Daesan petrochemical plumes, including estimates of emission factors, will be presented in a companion paper by Fried et al. (2020). We also estimate the ozone formation potential (OFP) of the VOCs measured over Seoul and identify the major VOC sources that impact Seoul using source apportionment and other techniques. These VOC sources are compared with the KORUS-AQ emission inventory (EI). Finally we discuss strategies to reduce emissions of the most reactive VOCs in Seoul.

## 2. Methods

### *2.1. KORUS-AQ mission overview*

The KORUS-AQ mission included 20 local science flights aboard the NASA DC-8 research aircraft, which was based at the Osan Air Base about 50 km south of Seoul (*Al-Saadi et al.*, 2015; *Crawford et al.*, 2020). The flights occurred from May 2 to June 10, 2016 (local Korean time) and were typically about 8 hours long for a total of 154 flight hours.

#### 2.1.1. Meteorological conditions

The 6-week KORUS-AQ mission was influenced by four major synoptic weather patterns (*Peterson et al.*, 2019; **Table 1**). The dates below are based on local Korean time (UTC + 9 hrs):

(1) May 2–15: *Dynamic period* featuring the passage of five strong frontal boundaries through the study region, large vertical motion, rapid storm movement, and winds generally from the W to N.

**Table 1: Synoptic-scale meteorological conditions for 20 research flights based out of Osan, South Korea during KORUS-AQ (May 2–June 10, 2016).** Day of Year (DoY) and dates are based on local time (Korea Standard Time = UTC + 9 hrs). Flight notes indicate the main jetways that were flown by the NASA DC-8, as shown in Figure 1. DOI: https://doi.org/10.1525/elementa.434.t1

| Flight | DoY | Date | Meteorology | Features | Flight notes |
|---|---|---|---|---|---|
| 1 | 118 | April 27 | n/a | n/a | Transit flight |
| 2 | 123 | May 2 | Dynamic | Pollution transport | Seoul-Jeju |
| 3 | 125 | May 4 | Dynamic | Pollution transport | Seoul-Jeju, West Sea[a] |
| 4 | 126 | May 5 | Dynamic | Pollution transport | Seoul-Jeju |
| 5 | 128 | May 7 | Dynamic | Pollution transport | Seoul-Busan |
| 6 | 132 | May 11 | Dynamic | Pollution transport | Seoul-Jeju, Jeju-Busan |
| 7 | 133 | May 12 | Dynamic | Pollution transport | West Sea, East of Seoul |
| 8 | 134 | May 13 | Dynamic | Pollution transport | West Sea, SE Korea |
| 9 | 138 | May 17 | Stagnant | Local pollution | Seoul-Busan, Seoul-Jeju[b] |
| 10 | 139 | May 18 | Stagnant | Local pollution | Seoul-Busan, West Sea |
| 11 | 141 | May 20 | Stagnant | Local pollution | Seoul-Busan |
| 12 | 143 | May 22 | Stagnant | Local pollution | Seoul plume (E wind)[c] |
| 13 | 146 | May 25 | Transport | Extreme pollution | West Sea |
| 14 | 147 | May 26 | Transport | Extreme pollution | Seoul-Jeju |
| 15 | 151 | May 30 | Transport | Extreme pollution | West Sea, Seoul-Busan |
| 16 | 152 | May 31 | Transport | Extreme pollution | West Sea, Seoul-Jeju |
| 17 | 154 | June 2 | Blocking | Local pollution | Seoul-Jeju, Seoul-Busan, Daesan |
| 18 | 155 | June 3 | Blocking | Local pollution | Seoul-Jeju, Seoul-Busan, Daesan |
| 19 | 157 | June 5 | Blocking | Local pollution | Daesan[d] |
| 20 | 161 | June 9 | Blocking | Local pollution | Seoul-Jeju |
| 21 | 162 | June 10 | Blocking | Local pollution | Seoul-Jeju, Seoul-Busan |
| 22 | 166 | June 14 | n/a | n/a | Transit flight |

[a] Flight tracks shown in Figure 1b.
[b] Flight tracks shown in Figure 1c.
[c] Flight tracks shown in Figure 1d.
[d] Flight tracks shown in Figure 1e.

(2) May 16–23: *Stagnant period* under a persistent anticyclone that resulted in light wind speeds, warm surface temperatures, and minimal impact from long-distance transport, with winds from the ESE, when they were strong enough to measure.
(3) May 24–31: *Second transport period* following a frontal passage on May 24, with a return to dynamic conditions but featuring weaker frontal boundaries, slower storm movement, and reduced vertical motion when compared with the first dynamic period. Persistent flow from the WSW supported transport of air from China in a moist boundary layer, ultimately influencing some of the worst pollution and visibility restrictions observed during campaign.
(4) June 1–10: *Rex blocking pattern* that resulted in minimal pollution transport and the general dominance of local pollution sources, but featured larger variations in wind speed and direction when compared with the previous stagnant period. The flights on June 9 and 10 were not technically associated with blocking, since a weak front reached the study region on June 8, but there was not a major pattern change in its wake.

The KORUS-AQ study occurred during neutral El Niño/Southern Oscillation (ENSO) and near-neutral Arctic Oscillation (AO) conditions. The average meteorology during KORUS-AQ was therefore representative of a 30-year climatology for this region in late spring (*Peterson et al.*, 2019).

#### 2.1.2. Flight tracks

Each of the 20 research flights had a different flight track that best accommodated the research objectives according to the meteorological conditions (**Figure 1**). During periods of transport the aircraft often flew a north-south flight track over the West Sea to sample outflow from

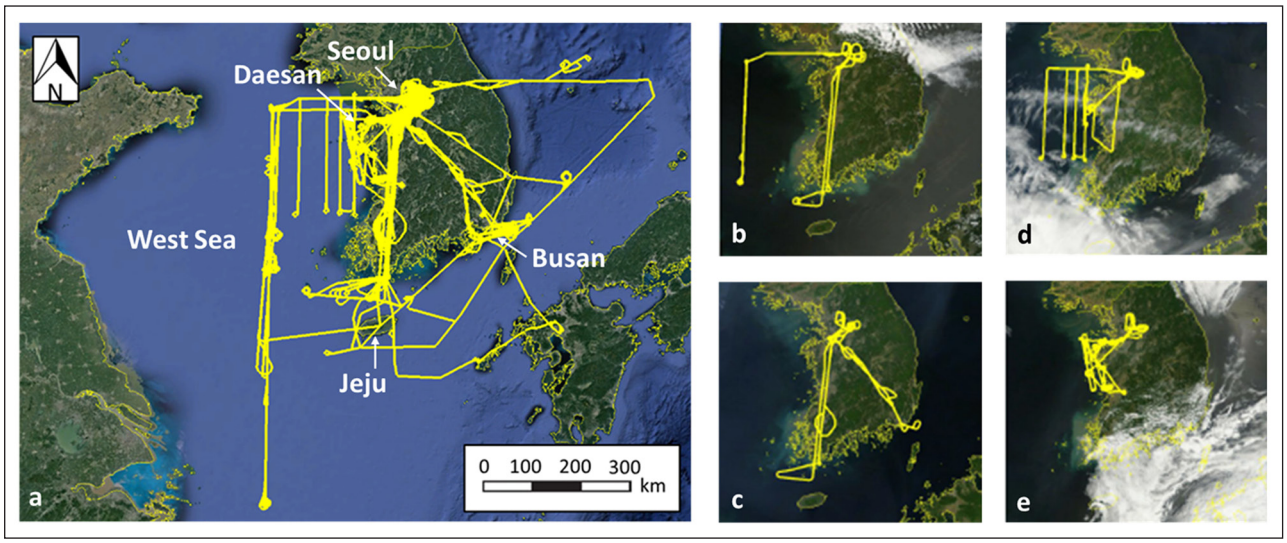


**Figure 1: Flight tracks of the NASA DC-8 research aircraft during the KORUS-AQ mission. (a)** All 20 local science flights from May 2 to June 10, 2016. **(b)** Flight 3 on May 4: West Sea and Seoul-Jeju jetways. **(c)** Flight 9 on May 17: Seoul-Jeju and Seoul-Busan jetways. **(d)** Flight 12 on May 22: Seoul plume and point source sampling under easterly winds. **(e)** Flight 19 on June 5: Point source survey of industrial sites near Daesan. The routine Seoul stereo routes are visible in the northeast flight tracks of panels (b–e). DOI: https://doi.org/10.1525/elementa.434.f1

China in isolation from Korean air (**Figure 1b**). Most flights included a Seoul-Jeju or Seoul-Busan jetway to capture air masses over the southern portion of the Korean peninsula (**Figure 1c**). With the exception of Flight 13, all flights also included a Seoul standard route or "stereo route" that was repeated over Seoul, with a missed approach over the Seoul Air Base in Seongnam (about 15 km southeast of Seoul) that allowed the aircraft to fly at low altitude over Seoul (100–1000 m), including Olympic Park in central Seoul (**Figure 1d**). All flights occurred during the daytime, and the Seoul stereo route was typically flown for 15–45 minutes near the beginning, middle and end of each flight (8 a.m., noon and 3 p.m. local time, respectively), allowing for comprehensive sampling of air over Seoul (*Nault et al.*, 2018). The example in **Figure 1d** also shows downwind sampling of the Seoul plume and point source emissions under an easterly wind. Three flights also targeted industrial sites near Daesan about 30 km southwest of Seoul (**Figure 1e**).

### *2.2. Airborne sampling*

#### 2.2.1. Whole air sampling (WAS)

A total of 2554 whole air samples were collected during the 20 research flights of KORUS-AQ, for an average of 128 samples per flight. Each air sample was collected during a 20 s to 3 min fill time into an electropolished, 2-L conditioned stainless steel canister equipped with a Swagelok Nupro metal bellows valve. The average fill time was 40 s and the longest fill times were at the highest altitudes (11 km). To collect an air sample an operator manually opened the valve, allowing a dual-head metal bellows pump to draw air from outside the aircraft into a ¼" forward-facing inlet, through an air sampling manifold and into the selected canister until it was filled to 40 psig (roughly 3 atm or 2000 Torr), at which time the valve was closed. Samples were collected on average every 3.5 mins. The average ± 1σ pressure altitude of the WAS samples was 2.0 ± 2.1 km, and the median altitude was 1.1 km. At the completion of each flight, the filled canisters were offloaded and couriered to UCI for laboratory analysis (Section 2.3).

The procedures to clean and prepare each canister for field use are described in Simpson et al. (2010). Briefly, the canisters were first conditioned by baking them in humidified air at 225°C for 12 hr in order to form an oxidative layer inside the canisters that passivates the canister walls. Next, after a series of pump-and-flush procedures in clean mountain air, the canisters were evacuated to $10^{-2}$ Torr, filled to 1000 Torr with ultra-high purity helium, evacuated once again to $10^{-2}$ Torr, then humidified by adding 17 Torr of purified water (the approximate vapour pressure of water at room temperature) in order to minimize surface adsorption.

The airborne KORUS-AQ samples were supported by limited ground-based whole air sampling in Seoul in spring 2015 ($n$ = 23), a year before KORUS-AQ during the Megacity Air Pollution Study-Seoul (MAPS-Seoul) campaign (*H. Kim et al.*, 2018b; *S. Kim et al.*, 2016, 2018). The samples were collected into evacuated 2-L canisters (the same canisters as described above) at 09:30 and 15:00 local time on most days from May 23–39 and June 3–10 at the Korean Institute for Science and Technology (KIST; 37.60°N; 127.04°E), at a site located 250 m southeast of a freeway and 150 m northwest of a research forest. The KIST samples were filled to ambient pressure over a sampling period of about 3 min. The canister preparation procedures and analysis at UCI were the same as for KORUS-AQ. Although limited, the ground-based measurements indicate whether the VOC results are robust from year-to-year and whether the low-altitude airborne observations during KORUS-AQ are generally consistent with ground-based measurements. Ground-based VOC measurements were also made by another research team during KORUS-AQ and will be reported separately.

#### 2.2.2. Fast-response instruments

The analysis in this paper also uses selected measurements from other KORUS-AQ teams using fast-response, real-time instruments (Tables S-1, S-2). All fast-response measurements were averaged over the longer fill time of the UCI WAS samples, called the WAS data merge, and these averages are used here. The calibration procedures for selected fast instruments are described in Section 1 of the Supplemental Material (SM).

(1) Several VOCs and OVOCs were measured using a proton-transfer-reaction time-of-flight mass spectrometer (PTR-ToF-MS) at 1 Hz frequency (*Müller et al.*, 2014). While some PTR-ToF-MS OVOCs were reported as a combined measurement (acetone + propanal, MVK + MACR + ISOPOOH), others were reported separately and are presented here (methanol, acetaldehyde, methyl ethyl ketone or MEK; Table S-2). However, while MEK is free of interferences in remote regions, other species such as butanal could contribute to the signal in the Seoul region. The measurement precision depends on the signal integration time and the concentration. The precision at 3 ppbv is estimated to be 0.418 ppbv for methanol, 0.122 ppbv for acetaldehyde, and 0.087 ppbv for MEK. Toluene was measured by PTR-ToF-MS without interference, with a precision of 0.091 pptv at 3 ppbv. The reduced electric field strength (E/N, with E being the electric field strength and N being the gas density) in the drift tube was ~110 Td (1 Td = $10^{-17}$ V cm$^2$). Section 2 of the SM compares WAS and PTR-ToF-MS toluene measurements, which shows that data obtained using different techniques and independent calibration methods agree well (Figures S-1, S-2).

(2) Carbon monoxide and methane ($CH_4$) were measured using the NASA Langley Differential Absorption Carbon monoxide Measurement (DACOM), an *in situ* diode laser spectrometer system (*Warner et al.*, 2010). The DACOM time response is 1 s and the measurement precision is 0.1% for $CH_4$ and 1% for CO.

(3) Formaldehyde ($CH_2O$) was measured using a Compact Atmospheric Multispecies Spectrometer (CAMS) that uses mid-infrared laser light to detect $CH_2O$ with an overall uncertainty of 4–6% (*Richter et al.*, 2015; *Spinei et al.*, 2018). This instrument also acquired fast ethane measurements with a similar uncertainty range. The WAS and CAMS measurements of ethane are compared in Figure S-2.

(4) Nitric oxide (NO), nitrogen dioxide ($NO_2$), total reactive nitrogen ($NO_y$) and $O_3$ were measured using the NCAR 4-Channel $NO_{xy}O_3$ Chemiluminescence Instrument, which uses $O_3$ as a reagent to measure the nitrogen compounds, and NO as a reagent to measure $O_3$ (*Weinheimer et al.*, 1994). The precision is 1–5% for nitrogen compounds and 1% for $O_3$.

(5) Hydrogen cyanide (HCN) was measured using the Caltech Chemical Ionization Mass Spectrometry (CIMS) instrument, which measures the reaction product ion $CF_3O^-$·HCN at $m/z$ = 112 (*Crounse et al.*, 2009). HCN is measured at 1 Hz with a precision of 20 pptv and an accuracy of 30%.

### 2.3. Laboratory analysis of WAS VOCs

During KORUS-AQ the filled WAS canisters were analyzed within 7 days of collection. Each reported VOC has been tested to ensure that its growth or destruction in the canisters is negligible during the interval between sample collection and analysis (*Simpson et al.*, 2010) and the VOCs we report were stable in the canisters during transit. The canisters were analyzed at UCI using multi-column gas chromatography (GC) for 82 $C_1$–$C_{10}$ VOCs, namely 14 alkanes ($C_2$–$C_{10}$), 4 cycloalkanes ($C_4$–$C_7$), 10 alkenes ($C_2$–$C_{10}$), ethyne, 14 aromatics ($C_6$–$C_9$), 29 halocarbons ($C_1$–$C_2$), 8 alkyl nitrates ($C_1$–$C_5$), carbonyl sulfide (COS) and dimethyl sulfide (DMS). The limit of detection (LOD), measurement precision, accuracy and atmospheric lifetime of each VOC is given in Table S-2. The measurement precision is determined from replicate analyses of pontoons of air, and the values in Table S-2 are conservative. For example, the precision of toluene is 3% at lower values (~100 pptv) and 1% at higher values (~15,000 pptv), and so a conservative precision of 3% is given in Table S-2.

The detailed GC set-up and analytical procedures for the WAS measurements are described in Colman et al. (2001) and Simpson et al. (2010). During KORUS-AQ three Hewlett-Packard GCs (HP-6890) and five column/detector combinations were used with flame ionization detection (FID), electron capture detection (ECD) and a mass selective detector (MSD) operating in selected ion monitoring (SIM) mode. The five column/detector combinations were DB-1 + FID, PLOT/DB-1 + FID, Restek-1701 + ECD, Restek-1701/DB-5 + ECD, and DB-5 ms + MSD. Most compounds eluted with highest precision on one column/detector combination. When a high-precision peak eluted on two column/detector combinations the results were averaged (e.g., propane, propene, benzene, toluene, ethylbenzene, xylenes). Most hydrocarbons were measured with FID, except the pinenes, branched alkanes, and aromatics ≥C8, which were measured with MSD. Alkyl nitrates and most halocarbons were measured using ECD, except HFCs and HCFCs which were measured using MSD. COS and DMS were also measured using MSD. To analyze a sample, the canister was connected to the analytical system and 2410 cm$^3$ of sample air was passed through molecular sieve traps to remove contaminants. Target VOCs within the sample air were then cryogenically pre-concentrated as the sample air flowed over glass beads immersed in a liquid nitrogen cooled loop. The VOCs were volatilized when the loop was immersed in hot water, and then the VOCs were flushed into a helium carrier flow to a splitter box that separated the sample flow into five streams, each directed to one of the column/detectors. The detector signal was digitally recorded and each chromatographic peak was individually inspected and manually integrated in order to increase the precision.

The UCI group has been making VOC measurements since the late 1970s and early 1980s, and our calibration standards and procedures date back to this time (*Colman*

*et al.*, 2001; *Simpson et al.*, 2010). For hydrocarbons we use a 0.99 ppm propane standard purchased in 1978 from the National Bureau of Standards (NBS, now the National Institute for Science and Technology or NIST) to calculate our per carbon response factor (PCRF), which converts detector response in area units to mixing ratios. This PCRF is compared to those calculated from less expensive commercial NIST and Scott-Marrin standards, and then the PCRFs from propane to decane are assigned based on the less expensive standards. The UCI halocarbon standards are either NIST-traceable or were made in-house from static dilutions prepared at UCI. The hydrocarbon and halocarbon measurements agree well with those from other laboratories in both formal and informal comparison experiments (*Apel et al.*, 2003; *Hall et al.*, 2014; *Hornbrook et al.*, 2011). The calibration procedures for the WAS measurements are further described in Section S1 and Table S-1 of the SM.

### *2.4. Source apportionment*

Major VOC sources in Seoul were investigated using Positive Matrix Factorization (PMF), a widely used multivariate receptor modeling technique (*Brown et al.*, 2015; *Hopke*, 2016; *Norris et al.*, 2014; *Paatero et al.*, 2014). Here we used the U.S. Environmental Protection Agency (EPA) PMF Version 5.0 (*Norris et al.*, 2014). The PMF program decomposes an $m \times n$ matrix ($x_{ij}$) of sample data—in this case the mixing ratios of $n$ = 21 VOCs measured in $m$ = 177 samples collected at low altitude over Seoul (Section 3.3.2)—into two matrices called factor contributions (G) and factor profiles (F). The factor contributions express the mass or percent contribution of each factor to the measured concentration of each VOC. The factor profiles are species profiles and need to be interpreted by the user based on their existing knowledge of VOC source profiles, in our case using experience together with relevant VOC profiles from the literature (e.g., *Du et al.*, 2016; *Guo et al.*, 2011a, b; *Kwon et al.*, 2007; *McDonald et al.*, 2018; *Na et al.*, 2004; *Ou et al.*, 2015; *Tang et al.*, 2014; *Wang et al.*, 2014). The chemical mass balance equation is expressed as (*Norris et al.*, 2014):

$$x_{ij} = \sum_{k=1}^{p} g_{ik} f_{kj} + e_{ij} \qquad \text{(Eq. 1)}$$

where $g$ is the mass contributed by each factor, $f$ is the species profile of each factor, $e_{ij}$ is the residual for each VOC $j$ in each sample $i$, and $p$ is the number of factors. The user chooses the number of factors that the PMF program will output. Here we ran PMF solutions for $k$ = 3–6 factors and the results are discussed in Section 3.3.2.

The PMF factor contributions and factor profiles are derived by minimizing the "goodness of fit" or objective function Q, which is a critical parameter for PMF (*Bon et al.*, 2011; *Brown et al.*, 2015; *Norris et al.*, 2014):

$$Q = \sum_{i=1}^{m} \sum_{j=1}^{n} \left[ \frac{x_{ij} - \sum_{k=1}^{p} g_{ik} f_{kj}}{u_{ij}} \right]^2 = \sum_{i=1}^{m} \sum_{j=1}^{n} \left[ \frac{e_{ij}}{u_{ij}} \right]^2 \qquad \text{(Eq. 2)}$$

where $u_{ij}$ is the estimated uncertainty of each VOC in the sample matrix. Here the uncertainty matrix was constructed using the precision of the VOC concentration within each sample (Table S-2), and an extra modeling uncertainty of 20% was added when the model was run. For example, a toluene value of 1531 pptv at a precision of 3% was assigned an uncertainty of 1531 × 0.03 = 46 pptv in the uncertainty matrix. Because the precision values are conservative (Section 2.3), the uncertainty is overestimated for some mixing ratios. Of the 21 × 177 = 3717 data points in the sample matrix, only three (two *n*-heptane samples and one isoprene sample) were below their limit of detection (LOD). They were assigned a value of 5/6 the LOD (so 2.5 pptv) and their uncertainty was assigned as 50% (so 1.5 pptv) (*Norris et al.*, 2014). PMF calculates a value called Q(true) using all the data points in the sample matrix, and a value called Q(robust) by excluding data points with uncertainty-scaled residuals ($e_{ij}/u_{ij}$) > 4 (*Norris et al.*, 2014). Here Q(true) and Q(robust) had the same value because the scaled residuals were all <4. This means that even though PMF was operated in its "robust mode", which automatically downweights the impact of samples with scaled residuals >4, this was not an issue here.

The PMF model offers several ways to understand the viability of the PMF solution and the correct number of factors to choose. This includes classic bootstrap (BS), displacement of factor elements (DISP), and bootstrap enhanced by displacement (BS-DISP), which are complementary ways to estimate the random errors and rotational ambiguity of the factor solutions (*Brown et al.*, 2015). PMF also calculates a value called Q/Q(expected), or Q/Qexp, which is >2 when a species is not well modeled by the PMF solution (*Norris et al.*, 2014). These PMF error estimation methods are applied in Section 3.3.2. Previous field studies have further discussed the uncertainties and limitations of PMF (e.g., *Bon et al.*, 2011; *Gao et al.*, 2018; *Yuan et al.*, 2012). For example, Bon et al. (2011) used PMF to identify three dominant factors in a study of VOC sources in Mexico City, and cautioned that more PMF factors caused major factors to be split rather than identifying separate minor emission sources. The uncertainties and limitations of the PMF analysis are discussed in Sections 3.3.2 and 3.3.3.

### *2.5. KORUS-AQ emission inventory*

The VOC sources inferred for Seoul using PMF were compared with the KORUS-AQ version 5 (KORUSv5) emission inventory for 2015, which was developed at Konkuk University and is a modified version of the official Korean EI called Clean Air Policy Support System (CAPSS) for South Korea (*Lee et al.*, 2011). The KORUSv5 EI geographically covers all of Asia and uses the Sparse Matrix Operator Kernel Emissions (SMOKE-Asia) emissions processing (*Woo et al.*, 2012) and SAPRC-99 chemical mechanism (*Carter et al.*, 2000). The inventory reports CO, $NH_3$, $NO_x$, $PM_{2.5}$, $PM_{10}$, $SO_2$ and VOCs on a 3 km grid resolution for South Korea, and does not include biogenic VOC sources. The VOCs are based on 30 VOC groups including 12 VOC groups measured in common with WAS, namely 5 alkane/alkyne groups, 5 alkene groups and 2 aromatic groups that are based on reactivity. The VOCs measured in common with WAS

account for 98% of the KORUSv5 VOC emissions, with OVOCs comprising the remaining 2%.

### *2.6. Back trajectory analysis*

Back trajectories along selected flight tracks were calculated using the Lagrangian FLEXible PARTicle dispersion model (FLEXPART) version 9.0.3 (*Stohl et al.*, 2005; https://www.flexpart.eu). 25,000 particles were released per trajectory calculation to estimate air mass history and uncertainty. The 48-hour backward simulations were driven by 3 hourly wind fields from the National Centers for Environmental Prediction (NCEP) Global Forecast System (GFS) model on a 0.25° × 0.25° grid.

### *2.7. CAM-chem model simulations*

Global model simulations of tropospheric chemistry, as well as CO-like tracers from various regions for the KORUS-AQ period were performed using the Community Atmosphere Model with chemistry (CAM-chem; *Tang et al.*, 2019). CAM-chem is a configuration of the global Community Earth System Model (CESM) with detailed tropospheric and stratospheric chemistry (*Tilmes et al.*, 2015). The results shown here are from a simulation at 0.5° horizontal resolution and are nudged to meteorological reanalysis fields from the Modern-Era Retrospective analysis for Research and Applications, Version 2 (MERRA-2).

## 3. Results & discussion

### *3.1. VOC distributions and source signatures*

#### 3.1.1. General mission overview

The air samples collected during KORUS-AQ showed distinct VOC distributions and signatures depending on their source origins. The spatial distributions of three VOC tracers are shown in **Figure 2** as an example. Isoprene, a short-lived biogenic tracer (*Guenther et al.*, 2012) was elevated over less populated areas of Korea along the Seoul-Jeju and Seoul-Busan flight tracks (**Figure 2a**). Toluene, an urban tracer (*Guo et al.*, 2006), was primarily elevated over the SMA in northwest Korea, with mixing ratios up to 10.4 ppbv during the missed approach over Seoul (**Figure 2b**; **Table 2**). By contrast, COS, which has sources

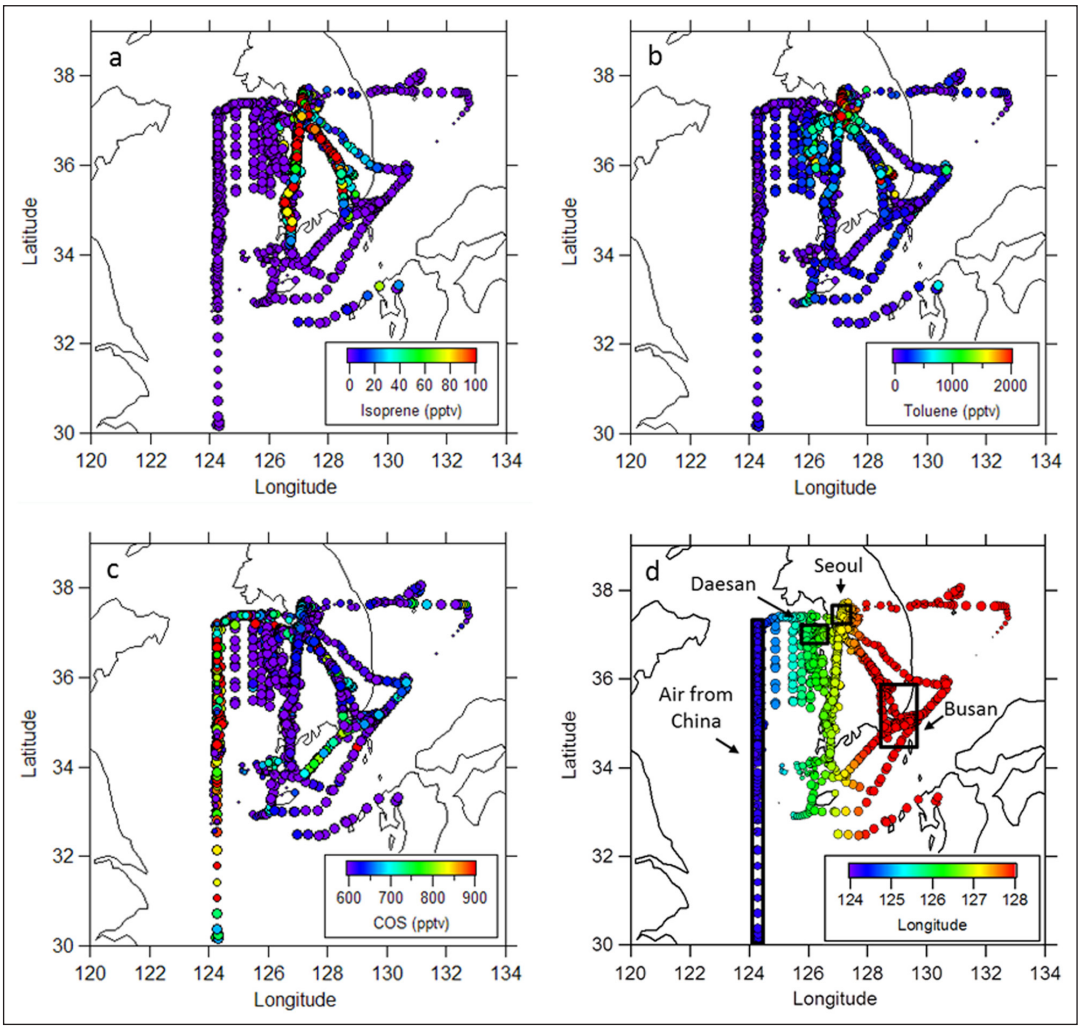


**Figure 2: Spatial distributions of selected VOCs during KORUS-AQ. (a)** Isoprene, a short-lived biogenic tracer, was most enhanced over the Korean land surface. **(b)** Toluene, an urban solvent tracer, was most elevated over the Seoul Metropolitan Area (SMA). **(c)** Carbonyl sulfide (COS), which has sources including coal combustion and $CS_2$ oxidation, was most enriched in air arriving from China. **(d)** Locations of source regions of interest during KORUS-AQ, including Seoul (yellow), Daesan (green), the Busan region (red), and air arriving from China (blue). Panels (a)–(c) are colour-coded by mixing ratio, and panel (d) by longitude. DOI: https://doi.org/10.1525/elementa.434.f2

**Table 2: Top 20 most abundant VOCs and OVOCs measured aboard the NASA DC-8 during KORUS-AQ at altitudes <500 m (1) over the Seoul Metropolitan Area ($n$ = 177), (2) in plumes from the Daesan petrochemical facility ($n$ = 63) and (3) in air masses originating from China ($n$ = 68).** The VOCs were measured using WAS, $CH_2O$ was measured using CAMS, and OVOCs were measured using PTR-ToF-MS. The fast-response $CH_2O$ and OVOC measurements were averaged over the WAS sampling times. Note that values have not been rounded and in many cases are presented beyond their level of significance (the measurement precision of each compound is shown in Table S-2). Min = minimum; max = maximum; med = median, avg = average, std = standard deviation, COS = carbonyl sulfide, DCE = dichloroethane, Me = methyl, MEK = methyl ethyl ketone. Units are pptv. DOI: https://doi.org/10.1525/elementa.434.t2

| Rank | Seoul | | | | | | Daesan | | | | | | China | | | | | |
|---|---|---|---|---|---|---|---|---|---|---|---|---|---|---|---|---|---|---|
| | Compound | Min (pptv) | Max (pptv) | Med (pptv) | Avg (pptv) | Std (pptv) | Compound | Min (pptv) | Max (pptv) | Med (pptv) | Avg (pptv) | Std (pptv) | Compound | Min (pptv) | Max (pptv) | Med (pptv) | Avg (pptv) | Std (pptv) |
| 1 | Methanol | 5368 | 68463 | 18928 | 21150 | 10354 | Methanol | 6756 | 28260 | 15915 | 15984 | 4355 | Methanol | 1181 | 35511 | 11433 | 12171 | 7093 |
| 2 | $CH_2O$ | 1237 | 9936 | 3835 | 3988 | 1681 | $CH_2O$ | 1275 | 18656 | 5905 | 7077 | 4255 | Ethane | 1078 | 3655 | 2354 | 2337 | 603 |
| 3 | Ethane | 1636 | 8727 | 2790 | 3200 | 1327 | Ethene | 40 | 26453 | 2578 | 5608 | 7240 | $CH_2O$ | 885 | 6393 | 1885 | 2173 | 1220 |
| 4 | Propane | 488 | 7683 | 2128 | 2309 | 1425 | Propane | 399 | 62536 | 2642 | 5383 | 8927 | Acetaldehyde | 381 | 4460 | 1040 | 1257 | 870 |
| 5 | Toluene | 117 | 10420 | 1981 | 2284 | 1832 | Acetaldehyde | 495 | 9546 | 2672 | 3361 | 2348 | Propane | 134 | 3701 | 772 | 1097 | 876 |
| 6 | Acetaldehyde | 418 | 5104 | 2114 | 2196 | 999 | Ethane | 1619 | 9105 | 2994 | 3313 | 1538 | Ethyne | 264 | 2839 | 974 | 1070 | 603 |
| 7 | MEK | 209 | 6854 | 1143 | 1461 | 1207 | *n*-Butane | 96 | 8416 | 1176 | 1858 | 1892 | $CH_3Cl$ | 603 | 2211 | 753 | 919 | 348 |
| 8 | *n*-Butane | 161 | 4914 | 1009 | 1262 | 949 | *n*-Hexane | 17 | 9694 | 639 | 1750 | 2213 | COS | 670 | 1512 | 868 | 914 | 196 |
| 9 | Ethyne | 304 | 2481 | 925 | 1026 | 490 | *i*-Butane | 50 | 13714 | 751 | 1720 | 2345 | CFC-12 | 510 | 555 | 526 | 526 | 8 |
| 10 | Ethene | 42 | 3366 | 714 | 870 | 676 | Benzene | 111 | 8011 | 853 | 1691 | 1889 | MEK | 101 | 2021 | 377 | 459 | 363 |
| 11 | HCFC-22 | 281 | 3759 | 742 | 865 | 549 | Propene | <LOD | 8497 | 404 | 1361 | 2120 | Benzene | 87 | 1350 | 397 | 454 | 298 |
| 12 | $CH_3Cl$ | 557 | 1208 | 715 | 752 | 146 | *i*-Pentane | 51 | 4972 | 937 | 1308 | 1293 | *n*-Butane | 14 | 2135 | 253 | 396 | 413 |
| 13 | *i*-Pentane | 89 | 3199 | 602 | 727 | 565 | $CH_3Cl$ | 561 | 6199 | 1011 | 1303 | 982 | $CH_2Cl_2$ | 88 | 938 | 339 | 365 | 186 |
| 14 | *i*-Butane | 78 | 2717 | 565 | 702 | 523 | Ethyne | 348 | 1939 | 925 | 988 | 405 | HCFC-22 | 259 | 807 | 311 | 358 | 113 |
| 15 | COS | 518 | 1082 | 651 | 698 | 138 | MEK | 159 | 1666 | 1105 | 979 | 429 | 1,2-DCE | 50 | 2517 | 220 | 354 | 423 |
| 16 | *m/p*-Xylene | 35 | 3747 | 369 | 538 | 602 | Toluene | 30 | 3894 | 887 | 974 | 750 | Ethene | 7 | 1394 | 115 | 259 | 352 |
| 17 | CFC-12 | 508 | 564 | 527 | 528 | 9 | *n*-Pentane | 32 | 3482 | 624 | 920 | 854 | *i*-Butane | 13 | 1281 | 147 | 254 | 260 |
| 18 | *n*-Pentane | 55 | 2266 | 401 | 518 | 424 | 3-MePentane | 3 | 5630 | 181 | 825 | 1137 | CFC-11 | 234 | 295 | 251 | 254 | 14 |
| 19 | $CH_2Cl_2$ | 81 | 1399 | 404 | 455 | 258 | COS | 547 | 1152 | 642 | 699 | 158 | Toluene | <LOD | 1645 | 102 | 249 | 359 |
| 20 | Ethylbenzene | 35 | 1691 | 370 | 432 | 352 | HCFC-22 | 248 | 1042 | 554 | 545 | 213 | *i*-Pentane | 6 | 1111 | 98 | 195 | 247 |

including domestic coal combustion and oxidation of $CS_2$ emitted from rayon production (*Campbell et al.*, 2015; *Du et al.*, 2016) was strongly enhanced in air sampled along the West Sea flight track, with mixing ratios up to 1.5 ppbv or more than double background values (**Figure 2c**; **Table 2**). Based on FLEXPART back trajectories and CAM-chem model simulations, the elevated COS levels measured over the West Sea originated from northeast China, including Shandong Peninsula and Hebei province (**Figure 3**). Overall, these results show that isoprene is a biogenic tracer for KORUS-AQ, toluene is one of the tracers of air from Seoul, and COS is a tracer of air masses originating from China. Enlarged spatial distributions for central areas of interest are shown in Figure S-3, including ethene which was strongly elevated at the Daesan petrochemical facility (Section 3.1.3).

In addition to surface spatial distributions, the VOC enhancements were inspected using altitude-concentration plots that were colour-coded by longitude to make the different source regions apparent, namely Seoul (yellow), Daesan (green), the Busan region (red), and air from China sampled over the West Sea (blue) (**Figure 4**). The latitude ranges of these different source regions are provided below and shown in **Figure 2d**. **Figure 4** shows where each VOC showed it maximum enhancement and how the mixing ratios compare from region to region. For example, even though ethene was clearly elevated in Seoul (yellow), its highest levels during KORUS-AQ were from the Daesan petrochemical facility (green) which produces ethene (**Figures 4g**, S3d). Additional time series plots show whether the elevated VOC concentrations occurred during stagnant and/or dynamic periods (**Figure 5**). Based on this analysis each source region showed specific and distinct VOC signatures, as discussed below (Sections 3.1.2–3.1.4).

#### 3.1.2. Seoul

Like toluene, many VOCs showed their strongest enhancements of the KORUS-AQ mission during the missed approaches over Seoul. These gases comprised mostly of $C_7$–$C_9$ aromatics and non-brominated halocarbons (**Figure 4a–d**) and their mixing ratios were typically highest during the stagnant periods (**Figure 5a–e**). The most abundant VOCs measured over Seoul by WAS were, in descending order by average mixing ratio, ethane, propane, toluene, *n*-butane and ethyne (**Figure 6b**). (The selection of the Seoul plumes is described in Section 3.2.1.) Similar results were found for the ground-based WAS measurements measured at KIST in 2015 (**Figure 6a**). When OVOCs are included, methanol was the most abundant VOC in Seoul, and the predominantly oxidation products formaldehyde and acetaldehyde were also in the top 10 species (**Table 2**). The ground-based measurements in Seoul in 2015 also found abundant methanol as well as acetone (*H. Kim et al.*, 2018). The Seoul VOC results are further discussed in Sections 3.2 and 3.3 in terms of ozone formation potential and VOC sources, respectively.

The Seoul results are also notable in terms of the behaviour of some halocarbons, in particular CFC-11 which is not declining in the atmosphere as quickly as expected based on the Montreal Protocol, with observational evidence for ongoing emissions from eastern Asia (*Montzka et al.*, 2018; *Rigby et al.*, 2019). During KORUS-AQ, while air originating from China was clearly elevated in CFC-11, stronger CFC-11 enhancements were measured over Seoul including during the stagnant periods (**Figures 4d, 5e**). This is different from other long-lived halocarbons such as CFC-113, CFC-114 and $CCl_4$, which were more elevated in air arriving from China and were not elevated over Seoul during stagnant periods (**Figure 5g–h**). Correlations

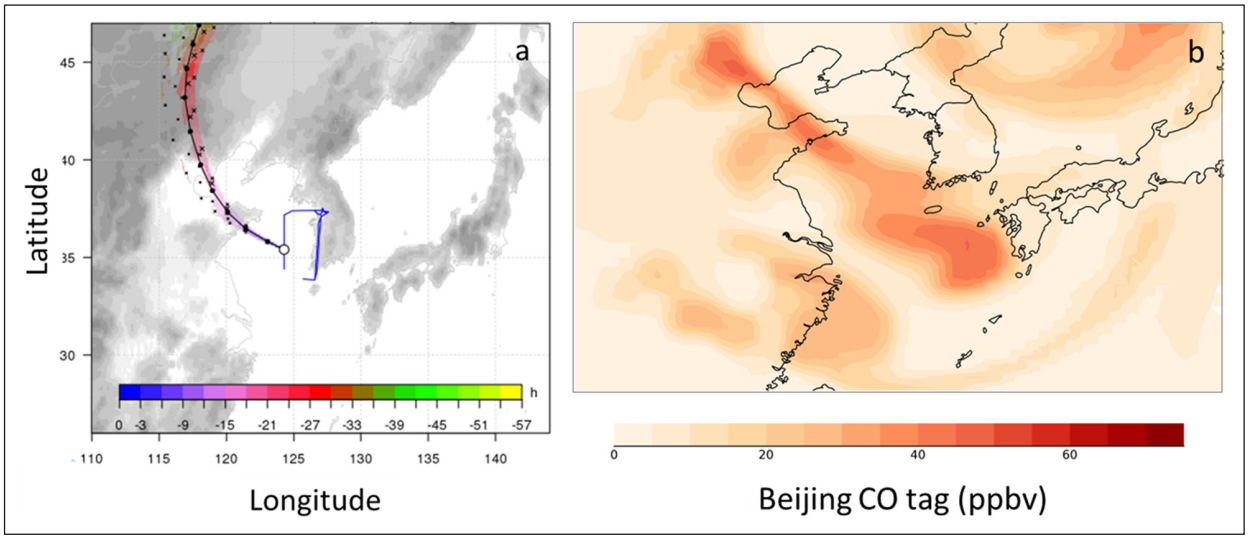


**Figure 3: FLEXPART back trajectories and CAM-chem model simulations during Flight 3 on May 4, 2016. (a)** FLEXPART back trajectories originating from 35.4°N, 124.3°E and 305 m AGL over the West Sea, plotted in 3-hour time steps from when the air mass was sampled at 10:00 local time (01:00 UTC). **(b)** CAM-chem model simulations of tagged CO from the Beijing region at 850 hPa (~1.5 km) on May 4. Flight 3 occurred during the first dynamic period and intercepted pollution from China, including some of the highest COS values of the mission. DOI: https://doi.org/10.1525/elementa.434.f3

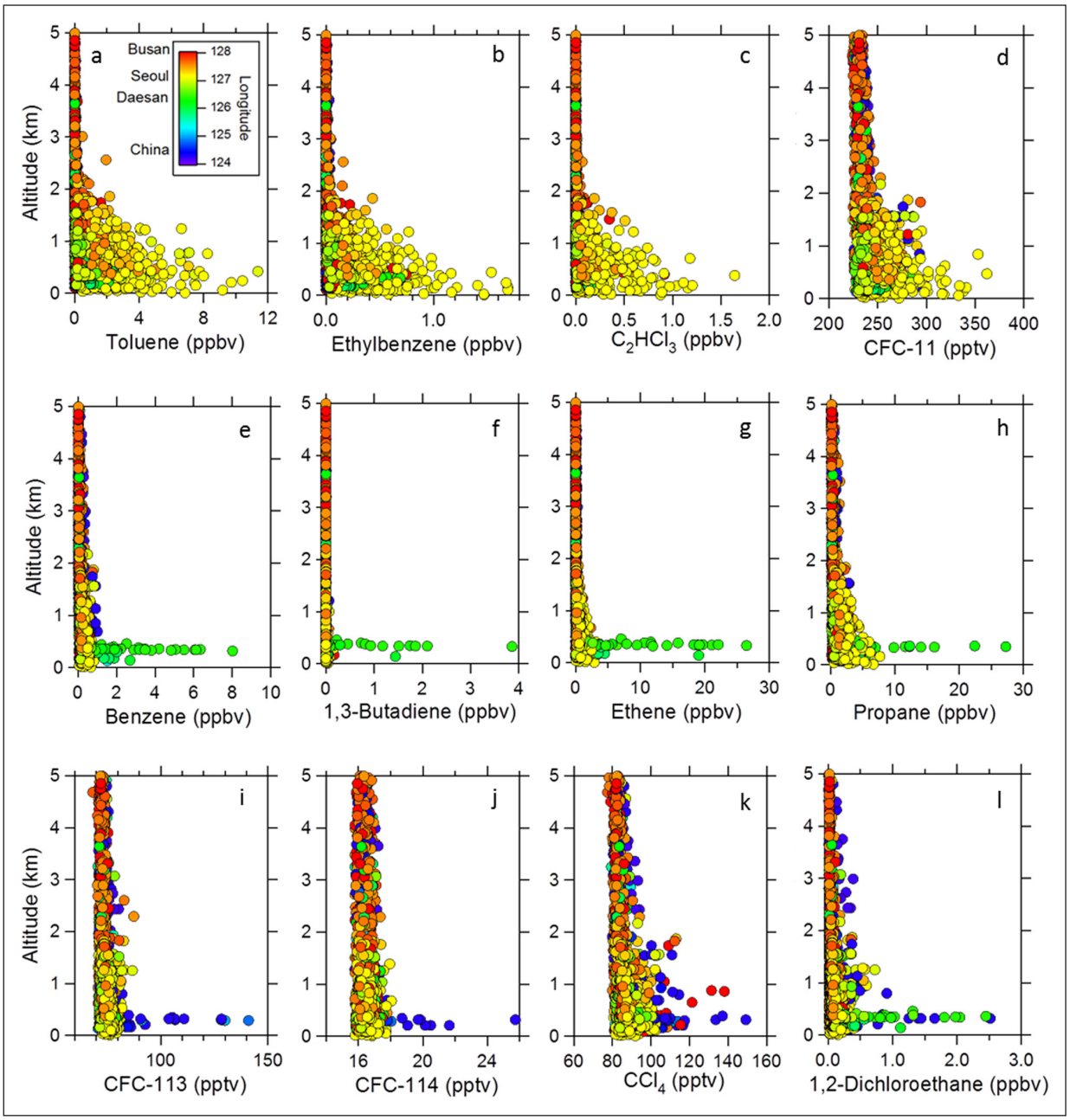


**Figure 4: Altitude distributions of selected VOCs measured by WAS during KORUS-AQ.** The mixing ratios are colour-coded by longitude: yellow = Seoul, green = Daesan petrochemical complex, blue = air masses originating from China, red = Busan. Elevated mixing ratios were observed for different VOCs in **(a–d)** Seoul, **(e–h)** Daesan, and **(i–l)** China. Some VOCs show multiple source regions, including $CCl_4$ (China and Busan) and 1,2-dichloroethane (China and Daesan). DOI: https://doi.org/10.1525/elementa.434.f4

between CFC-11 and China tracers such as $CCl_4$ and COS also show relatively elevated CFC-11 levels over Seoul compared to China ($CCl_4$ shown in **Figure 7a**). The CFC-11 enhancements over Seoul will be fully presented in a separate paper.

#### 3.1.3. Daesan

Whole air samples collected over the Daesan petrochemical complex showed a distinct chemical signature compared to VOCs collected over Seoul or in air arriving from China (**Figure 4e–h**). Of the 82 VOCs measured by WAS, 33 (or 40%) had their maximum values of the KORUS-AQ mission over the Daesan complex, including all alkanes, cycloalkanes and non-biogenic alkenes. Four of the 33 VOCs are either known carcinogens (benzene, 1,3-butadiene) or possible carcinogens (styrene, $CHCl_3$). The Daesan samples were selected for further analysis based on a geographic box that encloses 36.8–37.2°N, 125.9–126.5°W, and altitudes less than 500 m ($n = 63$). Based on this selection, the WAS Daesan samples were richest in ethene, $C_2$–$C_6$ alkanes and benzene (**Figure 6c**). Several OVOCs were also elevated in the Daesan plumes, including the highest levels of formaldehyde and acetaldehyde observed during the KORUS-AQ mission (**Table 2**). As noted in Section 1, the Daesan results will be fully presented in a companion paper by Fried et al. (2020).

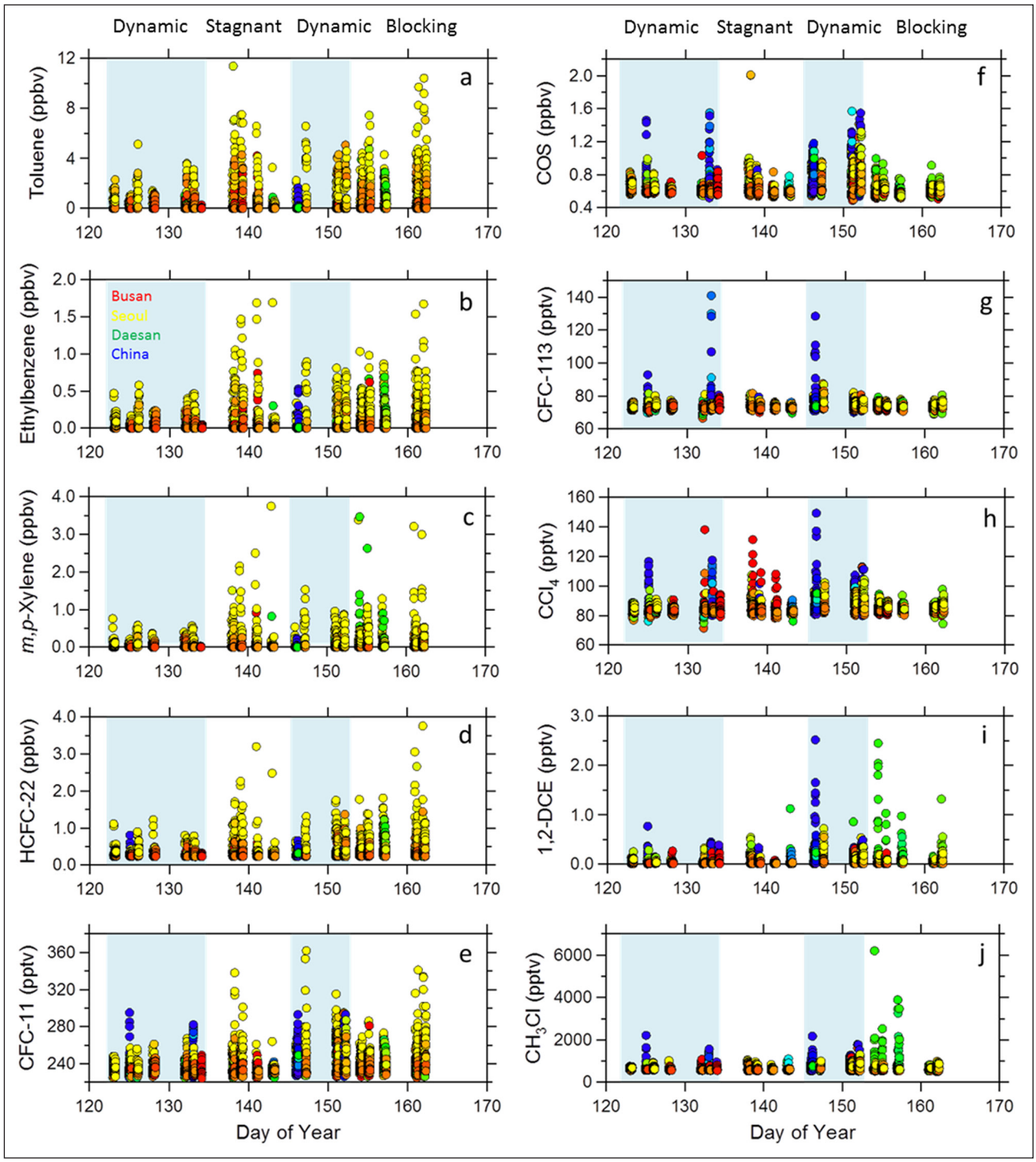


**Figure 5: Time series of selected VOCs measured by WAS during KORUS-AQ.** The mixing ratios are colour-coded by longitude as in Figure 4 (yellow = Seoul, green = Daesan, blue = China, red = Busan). VOCs shown in panels **(a–e)** were more elevated over Seoul, while VOCs in panels **(f–i)** were more elevated in air originating from China. Panel **(j)** shows $CH_3Cl$, which had its highest concentrations in industrial plumes from Daesan. Blue shading indicates dynamic conditions, supporting transport of air from China. White areas generally represent stagnant or blocking conditions, associated with minimal pollution transport. DOI: https://doi.org/10.1525/elementa.434.f5

#### 3.1.4. China

Because emission signatures from China evolve over time, each NASA airborne mission needs a new characterization of the current fingerprint of air from China. For example, during the 2001 Transport and Chemical Evolution over the Pacific (TRACE-P) mission, the fire suppressant Halon 1211 ($CF_2ClBr$) and the biomass burning tracer methyl chloride ($CH_3Cl$) were characteristic tracers of air from China (*Blake et al.*, 2003), and COS was also elevated in air from China (*Blake et al.*, 2004). A larger suite of gases (COS, $CH_3Cl$, 1,2-dichloroethane, ethyl chloride, Halon 1211) was recommended as tracers of air from China during the 2006 Intercontinental Chemical Transport Experiment, Phase B (INTEX-B; *Barletta et al.*, 2009). During

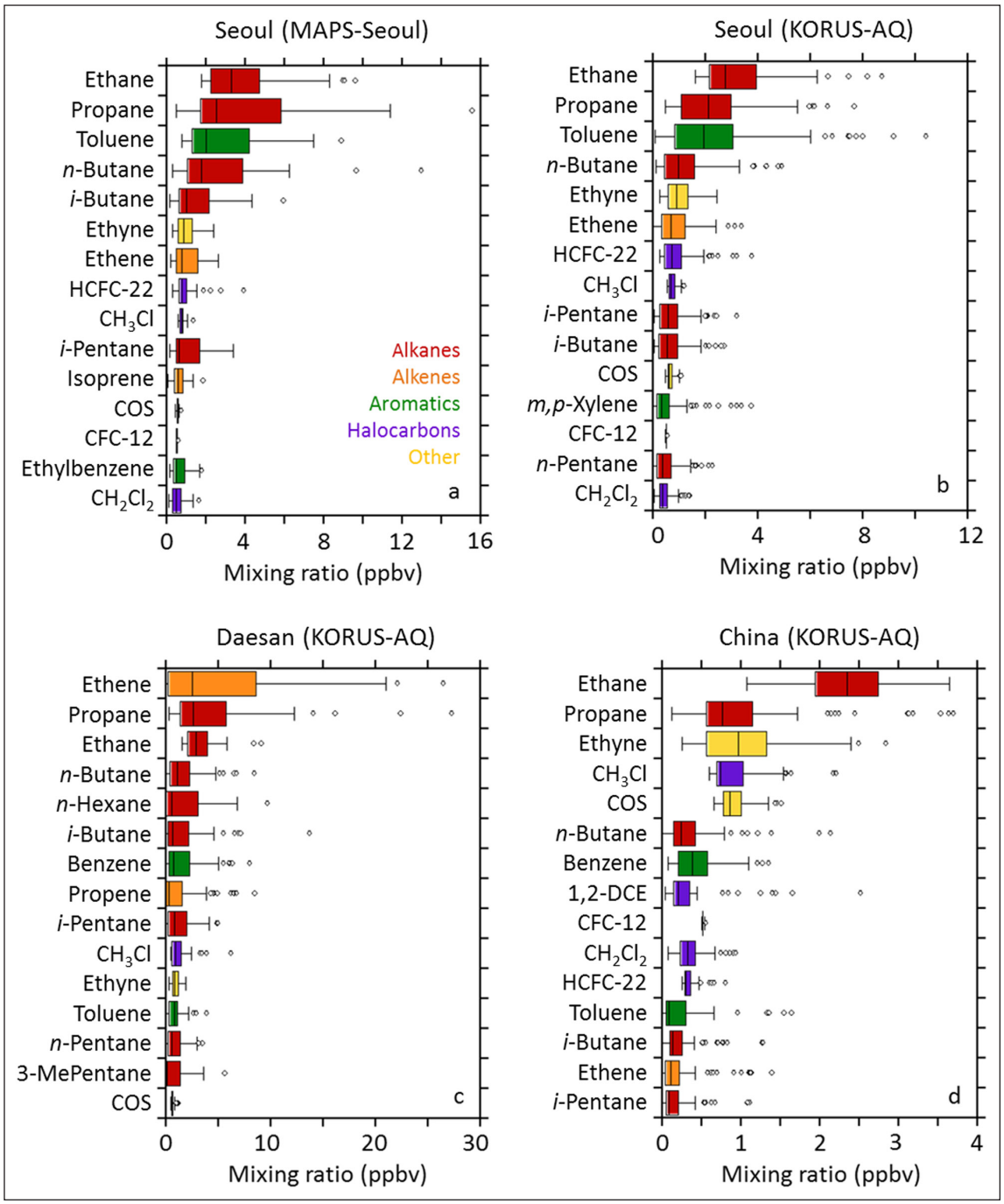


**Figure 6: Box-whisker plots of the 15 most abundant VOCs collected by WAS during the MAPS-Seoul and KORUS-AQ campaigns. (a)** Ground-based data collected at KIST in Seoul in May 2015 during MAPS-Seoul ($n = 23$). Low-altitude (< 0.5 km) airborne samples collected during KORUS-AQ over **(b)** Seoul, $n = 177$, **(c)** Daesan, $n = 63$ and **(d)** China, $n = 68$. The VOCs are plotted in descending order based on average mixing ratio. Note that a maximum Daesan propane value of 62.5 ppbv (Table 2) is not shown. The plots show the interquartile range (box), median (line), and full data (whiskers) with the exception of outliers (open circles), which are values greater than the third quartile plus 1.5 times the interquartile range. Mixing ratios are colour-coded by compound class for easier comparison among the panels (red = alkanes, orange = alkenes, green = aromatics, purple = halocarbons, yellow = other). DOI: https://doi.org/10.1525/elementa.434.f6

KORUS-AQ, COS, CFC-113, CFC-114, $CCl_4$ and 1,2-dichloroethane all had strongly elevated levels in air originating from China (**Figures 4i–l, 5f–i**), and we recommend these five compounds as tracers for China during KORUS-AQ. Notably absent from this list is Halon 1211, which used to be produced primarily in China until its production was phased out in 2006 (*Fraser et al.*, 1999; *Vollmer et al.*, 2009). During KORUS-AQ Halon 1211 showed minimal enhancements over background values in air originating from China, and instead was most enhanced over Seoul (**Figure 7b**). Therefore, unlike previous missions such as TRACE-P and INTEX-B, Halon 1211 is no longer a useful

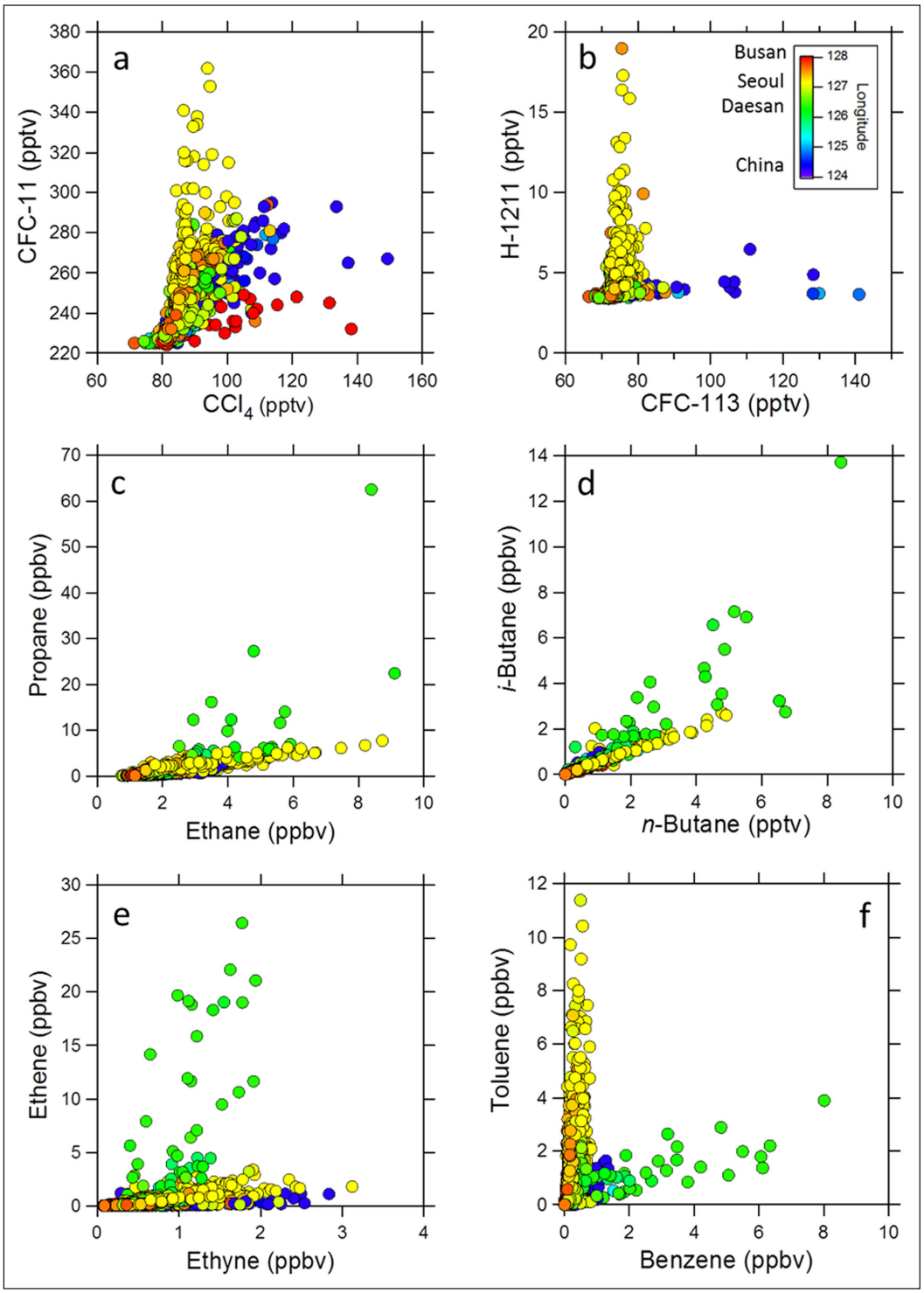


**Figure 7: Correlations among various VOCs tracers during KORUS-AQ. (a)** CFC-11 and $CCl_4$, **(b)** H-1211 and CFC-113, **(c)** propane and ethane, **(d)** *i*-butane and *n*-butane, **(e)** ethene and ethyne, **(f)** toluene and benzene. The mixing ratios are colour-coded by longitude as in Figure 4 (yellow = Seoul, green = Daesan, blue = China, red = Busan), with primary source regions shown in Figure 2d. DOI: https://doi.org/10.1525/elementa.434.f7

tracer of air from China. While $CH_3Cl$ was elevated in air from China during KORUS-AQ (up to 2.2 ppbv) and is still a tracer of air from China, it was much more elevated in the industrial Daesan plumes (up to 6.2 ppbv) (**Figure 5j**; **Table 2**).

The air samples originating from China and sampled at low altitude along the West Sea jetway were selected for further analysis based on a geographical box enclosing 30.2–37.4°N, 124.2–124.4°W and altitudes <500 m. The data were further selected to only include flights during dynamic periods, in other words flights 3, 7, 8, 13, 15 and 16 (**Table 1**), for a total of $n = 68$ samples. Of the 82 VOCs measured by WAS, these air samples were richest in ethane, propane, ethyne, $CH_3Cl$ and COS (**Figure 6d**). The air from China was also rich in primary and secondary OVOCs including methanol, formaldehyde and acetaldehyde (**Table 2**).

#### 3.1.5. Busan

A few halocarbons, notably $CCl_4$, H-2402 and HCFC-141b showed strong enhancements in southeast Korea near Busan ($CCl_4$ is shown in **Figures 4k, 5h**). The $CCl_4$ results have been presented in Lunt et al. (2018) and the remaining halocarbons will be addressed in a separate paper.

### *3.2. Ozone formation potential in Seoul*

VOCs react with nitrogen oxides ($NO_x$) in the presence of sunlight to form secondary products including $O_3$ and SOA. The potential of individual VOCs to form $O_3$ can be roughly characterized using reactivity scales such as OH reactivity ($k_{OH}$) and Maximum Incremental Reactivity (MIR). Because photochemically active VOCs are more efficient at forming $O_3$, policies based on ozone formation potential (OFP) are helpful for guiding VOC control measures, rather than measures based on VOC abundance (*Wu and Xie*, 2017). Below we investigate which VOCs are most effective at forming $O_3$ in Seoul.

#### 3.2.1. Selection and overview of Seoul data

The Seoul data used in this analysis were selected based on a geographical box around Seoul (37.3–37.7°N and 126.7–127.3°E) and low altitudes (<0.5 km), which yielded 177 samples that covered all four synoptic-scale meteorological conditions during the mission (Figure S-4). Importantly, this geographical boundary excluded the Daesan petrochemical facility since its VOC signature is distinct from that of Seoul (Section 3.1.3) and winds in Seoul were rarely from Daesan during KORUS-AQ (Section 2.1.1). Altitudes below 500 m were chosen to minimize the effects of transboundary sources on VOCs in Seoul (*Lamb et al.*, 2018; Section 4 of the SM). The average altitude of the Seoul data was 245 ± 126 m. Average atmospheric boundary layer heights in the Seoul region during spring, 2016 were 548 ± 180 m at night and 1182 ± 540 m during the day (H.-J. Lee et al., 2019). The earliest Seoul sample was collected at 7:40 a.m. Local Standard Time (LST), about 2 hours after sunrise, and the latest at 4:10 p.m. Therefore, while it is possible that a few higher-altitude samples closer to 500 m could have some impact from a more aged residual layer, especially early in the morning, most samples are expected to represent a well-mixed boundary layer.

Based on this data selection, OVOCs, alkanes and aromatics were most abundant in Seoul (Section 3.1.2). Excluding OVOCs, the contributions to VOC abundance (based on average mixing ratios for the 177 Seoul samples), were alkanes (46%), halocarbons (20%), aromatics (19%), alkenes (6%), alkynes (5%), sulfur compounds (3%) and alkyl nitrates (0.6%) (Figure S-5a). This is similar to previous work in South Korea which found that alkanes followed by aromatics were the largest contributors to VOC abundance in Seoul (halocarbons and OVOCs were not included; *Shin et al.*, 2013). When primary OVOCs without interference are included in the KORUS-AQ Seoul data (i.e., methanol), the weightings shift to methanol (51%), alkanes (23%), halocarbons (10%), aromatics (9%), alkenes (3%), alkynes (2.5%), sulfur compounds (2%) and alkyl nitrates (0.3%) (Figure S-5b). By comparison, the percentages for May data during the MAPS-Seoul campaign were OVOCs (57%), alkanes (29%), aromatics (9%) and alkenes (4%) (*H. Kim et al.*, 2018; halocarbons were not reported). That is, the overall percentages were similar during KORUS-AQ and MAPS-Seoul, though we note that the MAPS-Seoul data included speciated OVOCs besides methanol such as acetone.

#### 3.2.2. VOC impacts on ozone

The 'total' OH reactivity ($k_{OH}$, in $s^{-1}$) is a rough indicator of the potential of trace gases that react with OH to form $O_3$. In the case of VOCs, it is the product of VOC concentration ($[VOC_i]$, in molec $cm^{-3}$) and the rate coefficient for VOC reaction with OH ($k_{OH+VOCi}$, in $cm^3$ $molec^{-1}$ $s^{-1}$) (*Kovacs et al.*, 2003; *Yang et al.*, 2016):

$$k_{OH} = \sum_i^m k_{OH+VOCi}[VOC_i] \quad \text{(Eq. 3)}$$

Rate constants were taken from Atkinson and Arey (2003) and Atkinson et al. (2004, 2006, 2008), and average VOC mixing ratios over Seoul were used (Table S-2). Even though formaldehyde and acetaldehyde were present at appreciable mixing ratios in Seoul (Table S-2), they were not included in the $O_3$ analysis below because they were found to have a dominant photochemical source during KORUS-AQ (Schroeder et al., 2020).

VOCs that are both abundant and reactive with OH have a high potential to form $O_3$. For example during KORUS-AQ isoprene was a strong contributor to $k_{OH}$ in Seoul because it is reactive rather than abundant, whereas toluene was a strong contributor because it is abundant rather than reactive (Figure S-6). We note that *m,p*-xylene was a combined WAS measurement during KORUS-AQ, even though *m*-xylene and *p*-xylene have different reaction rate constants with OH and therefore different lifetimes (Table S-2), which is important for their individual $O_3$ formation potential and for policy considerations. However the *m*- and *p*-xylene isomers were speciated by WAS during MAPS-Seoul in 2015, and this information was used in the KORUS-AQ analysis. The average and median ratios of *m*:*p*-xylene during MAPS-Seoul were 471:318 and 344:231 pptv/pptv, respectively, or a ratio of about 3:2. This 3:2 ratio was used to speciate the KORUS-AQ *m,p*-xylene measurements for purpose of the OH reactivity calculations, in order to apply their different OH reaction rate constants. Because *m*-xylene was both more abundant and more reactive than *p*-xylene, it was a much stronger (~3×) contributor to OH reactivity in Seoul during KORUS-AQ (Figure S-6).

Of the VOCs measured by WAS, the strongest individual contributors to OH reactivity in Seoul were isoprene, toluene, *m*-xylene, ethene and propene (**Figure 8a**). Consistent with this, isoprene contributed most to daytime OH reactivity during MAPS-Seoul based on the ground-based WAS samples in spring 2015 (*S. Kim et al.*, 2018). We note that the contribution of isoprene to $k_{OH}$ in Seoul is expected to be lower in winter as compared to the spring timing of KORUS-AQ and MAPS-Seoul. Considering anthropogenic VOCs, the KORUS-AQ results are similar to Wu and

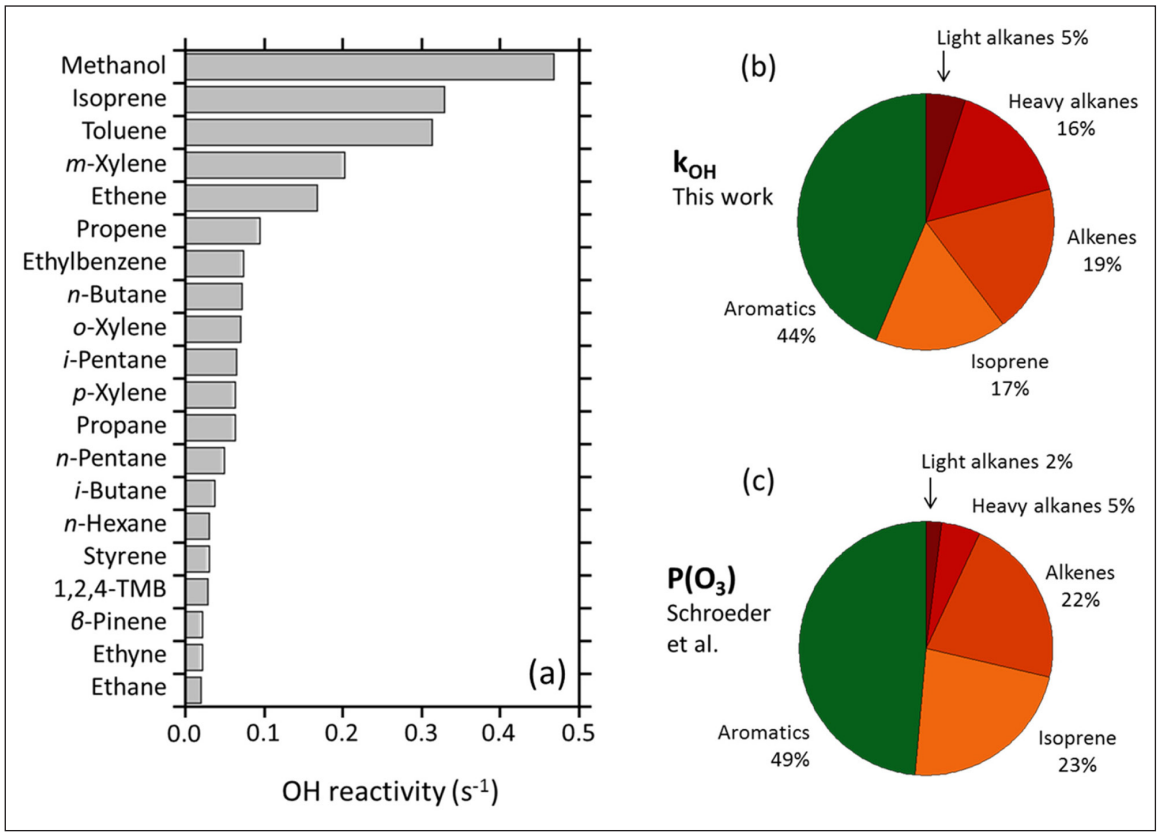


**Figure 8: OH reactivity and ozone production ($P(O_3)$) calculations for Seoul air samples during KORUS-AQ.** **(a)** OH reactivity in descending order for 20 primary VOCs and OVOCs collected at low altitude over Seoul ($n = 177$; alt. <0.5 km). Ozone formation potential by compound class based on **(b)** OH reactivity and **(c)** $P(O_3)$ calculations using photochemical box modeling, excluding methanol. 'Light alkanes' represents $C_2$–$C_3$ and 'heavy alkanes' are $C_4$ and higher. DOI: https://doi.org/10.1525/elementa.434.f8

Xie (2017), who found that the xylenes, ethene, toluene and propene had the largest potential to form $O_3$ in the major urbanized regions of China. Previous year-round VOC measurements in Seoul from 2004–2008 found that toluene, ethene, *n*-butane and propane were the main contributors to $O_3$ formation (*Shin et al.*, 2013). Although primary OVOCs such as methanol are not always measured in urban studies, the OH reactivity of methanol was higher than isoprene during KORUS-AQ (**Figure 8a**).

As a group, aromatics contributed most to VOC OH reactivity in Seoul during KORUS-AQ (44%), followed by non-isoprene alkenes (19%), isoprene (17%), heavy alkanes ≥$C_4$ (16%) and light $C_2$–$C_3$ alkanes (5%) (**Figure 8b**). These results show generally good agreement with 0-D photochemical box modeling estimates of $O_3$ production by VOCs over Seoul during KORUS-AQ, which were constrained by DC-8 observations (*Schroeder et al.*, 2020). The box model used zero-out simulations, whereby selected VOCs or VOC groups were removed from the model to test the model sensitivity to these VOCs. The model found that $O_3$ production in Seoul is VOC-limited and most sensitive to changes in aromatics, followed by isoprene and anthropogenic alkenes. For example, removing aromatics caused a 32% reduction in mean ozone production in the Seoul region, and removing isoprene and non-isoprene alkenes caused 15% and 14% reductions, respectively (*Schroeder et al.*, 2020). When expressed in pie chart format, to directly compare with the OH reactivity calculations, the model was most sensitive to aromatics (49%) followed by isoprene (23%), other alkenes (22%), heavy alkanes (5%) and light alkanes (2%) (**Figure 8c**). That is, the OH reactivity calculations and box modeling agreed in their major findings, namely the predominant impact of aromatics followed by alkenes in ozone formation in Seoul, with poorer agreement for heavy alkanes (16% and 5%, respectively). While the photochemical box modeling is more complex in its handling of radical chemistry, the OH reactivity calculations are able to give speciated VOC results (for example, the box model does not speciate the aromatics). The overall good agreement between the two suggests that results from the OH reactivity calculations can be reasonably used to identify which anthropogenic VOCs are most likely to form $O_3$ in Seoul and could be targeted for VOC emission reduction strategies (i.e., toluene, *m*-xylene, ethene).

The box modeling also assessed the impact of methanol on $O_3$ formation (*Schroeder et al.*, 2020). Removing methanol caused a 6% reduction in $O_3$ production in the zero-out calculations, or 8% when expressed as a pie chart together with the VOC groups (Figure S-7b). By comparison, methanol contributed 20% to OH reactivity based on VOCs + methanol (Figure S-7a). This suggests that the OH reactivity calculation over-weighted the contribution of methanol to ozone formation, most likely because it does

not take into account the subsequent radical chemistry in which methanol oxidation produces relatively less $O_3$ than a higher-chain molecule such as toluene.

### *3.3. VOC sources in Seoul*

VOC source influences can be diagnosed using a combination of techniques, both qualitative (e.g., presence of known VOC tracers, the ratio of one VOC to another, VOC correlations) and quantitative (e.g., source apportionment). We applied all these techniques to the KORUS-AQ WAS samples collected over Seoul, as discussed below.

#### 3.3.1. VOC tracers, ratios and correlations

The suite of VOCs measured during KORUS-AQ includes known tracers of both biogenic and anthropogenic sources that are relevant for Seoul.

*Biogenic:* Isoprene is a well-known biogenic tracer that also has a minor traffic source (*Borbon et al.*, 2001; *Guenther et al.*, 2012; *Khan et al.*, 2018). Here isoprene did not correlate with traffic tracers such as CO, ethene and 1,3-butadiene in the urban data, either in low-altitude Seoul data ($r^2 < 0.03$) or in the ground-based data at KIST ($r^2 < 0.02$), suggesting negligible impact of traffic on the isoprene emissions in Seoul. Other biogenic tracers such as $\alpha$- and $\beta$-pinene were minor during KORUS-AQ, with average mixing ratios <15 pptv (Table S-2). Methanol also has a major biogenic source (*Jacob et al.*, 2005; *Tie et al.*, 2003), although in the urban Seoul data methanol correlated much better with solvents such as ethylbenzene ($r^2$ = 0.78) than with isoprene ($r^2$ = 0.14), suggesting multiple source influences.

*Natural gas:* Ethane is a useful tracer of fossil fuel sources including natural gas (*Kille et al.*, 2019; *Smith et al.*, 2015). Natural gas is used for heating and cooking in South Korea, with five times more consumption in winter than in summer (*Na and Kim*, 2001; *Na et al.*, 2004). Residential natural gas is mostly methane (89% by mass), and its non-methane components are primarily ethane (71%), propane (22%) and the butanes (5%) (*Na et al.*, 2004). Natural gas is also used in South Korea's public transport sector, and all transit buses in Seoul have been fueled by CNG since 2010 (Section 1). During KORUS-AQ ethane and propane showed some correlation in Seoul ($r^2$ = 0.57) and the propane/ethane ratio was 0.99 ± 0.03 (**Figure 7c**). This 1:1 ratio is greater than the 1:3 ratio that would be expected if natural gas were the main source of ethane and propane, indicating other source impacts (Section 3.3.2). Likewise, while 1,3-butadiene has been reported in the exhaust of CNG-fueled buses (*Kado et al.*, 2005), 1,3-butadiene levels were low in both the airborne and ground-based Seoul samples (9 ± 19 and 24 ± 16 pptv, respectively).

*Liquefied petroleum gas (LPG):* Propane and the butanes are the major components of LPG. In South Korea propane-rich LPG (>90%) is used for residential and commercial cooking and heating, while butane-rich LPG mixed with 5–30% propane is used for autogas in taxis and other LPG-fueled vehicles (*KLPG*, 2004). Less propane is added to autogas in summer than winter, and the springtime autogas mix in Seoul would have about 95% butanes and 5% propane + other minor components (*Na et al.*, 2004). Industrial LPG in South Korea is rich in *i*-butane (>85%; *KLPG*, 2004). During KORUS-AQ the *i*-butane/*n*-butane ratio in Seoul was 0.53 ± 0.01 and the butanes showed excellent correlation ($r^2$ = 0.93; **Figure 7d**). Similar results were observed in the ground-based data at KIST (slope = 0.47 ± 0.02; $r^2$ = 0.98). An *i*-butane/*n*-butane ratio of around 0.5 is consistent with an LPG influence, whereas a lower ratio of 0.2–0.3 indicates biomass burning and a higher ratio of 0.6–1.0 can indicate natural gas (*Russo et al.*, 2010) or, in South Korea, use of industrial LPG. For example the *i*-butane/*n*-butane ratio in the industrial Daesan samples (1.08 ± 0.08; $r^2$ = 0.77) was richer in *i*-butane than the Seoul samples (**Figure 7d**). Overall, the butane ratios in Seoul point to impact from LPG rather than biomass burning, natural gas or industry.

*Gasoline evaporation:* Toluene, pentanes and methylpentanes are dominant species in gasoline evaporation (*Dai et al.*, 2013; *Wang et al.*, 2016; *Yue et al.*, 2017). Similar to the butanes, the pentanes are useful for distinguishing various combustion and fossil fuel sources, including gasoline evaporation. A *i*-pentane/*n*-pentane ratio around 0.5 indicates biomass burning (*Akagi et al.*, 2011), 0.8–1.0 represents oil and natural gas (*Abeleira et al.*, 2017; *Gilman et al.*, 2013), 1–3 suggests traffic (*Baker et al.*, 2008; *Fraser et al.*, 1998; *Na et al.*, 2006), and 3–4 indicates gasoline evaporation (*McGaughey et al.*, 2004; *Na et al.*, 2004; *Simpson et al.*, 2014). The *i*-pentane/*n*-pentane ratio in Seoul was 1.25 ± 0.03 ($r^2$ = 0.88), with similar results for the ground-based samples (1.34 ± 0.09; $r^2$ = 0.88), suggesting that gasoline evaporation is not a major influence in Seoul. By comparison, the *i*-pentane/*n*-pentane ratio in Mecca, Saudi Arabia, a city heavily impacted by gasoline evaporation, was 3.52 ± 0.02 (*Simpson et al.*, 2014). The pentane ratio in Seoul (1.25–1.34) is lower than traffic ratios in North America (2–3; *Baker et al.*, 2008; *Fraser et al.*, 1998) but similar to results from a Seoul tunnel study in 2000 (1.22–1.25; *Na et al.*, 2006).

*Vehicle exhaust:* Many VOCs are emitted in vehicle exhaust, with different emission profiles depending on fuel type. For example ethene, propene, aromatics and heavier alkanes are prominent in diesel exhaust (*Shen et al.*, 2018; *Tsai et al.*, 2012; *Wang et al.*, 2017; *Yao et al.*, 2015); light alkanes, light alkenes, toluene and benzene in gasoline exhaust (*Cao et al.*, 2016; *Guo et al.*, 2011a; *Wang et al.*, 2017); and propane and butanes in LPG exhaust (*Guo et al.*, 2011a). Among diesel-fueled vehicles, the proportion of alkenes is highest for light-duty diesel trucks followed by heavy-duty diesel trucks, with little alkene emission from light-duty diesel cars (*Wang et al.*, 2017). The ratio of ethene/ethyne helps to distinguish vehicle exhaust from other sources. The ethene/ethyne ratio is 1–3 for vehicle exhaust, with values <1 for older vehicles due to higher ethyne emissions, and >10 for petrochemical sources (*Pang et al.*, 2014; *Ryerson et al.*, 2003; *Simpson et al.*, 2014). During KORUS-AQ the ethene/ethyne ratio was 1.02 ± 0.07 in Seoul (and likewise 1.26 ± 0.13 for the ground-based Seoul samples) compared to 11.3 ± 1.9 in Daesan (**Figure 7e**), clearly showing their respective vehicular and industrial influences.

*Solvents:* Many cities in Asia are heavily impacted by solvents such as toluene (e.g., *Cai et al.*, 2010; *Guo et al.*, 2011b; *Song et al.*, 2018; *Li et al.*, 2019). Previous work in Seoul has also found an abundance of toluene (*Na et al.*, 2005; *Nguyen et al.*, 2009). The ratio of toluene to benzene (T/B) is a useful indicator of the relative impact of traffic versus solvents: a T/B ratio of 1–2 indicates traffic while >2 indicates solvent influence (*Barletta et al.*, 2005, 2017; *Wang et al.*, 2016). For example, based on measurements in the Pearl River Delta region of China, Liu et al. (2008) reported a T/B ratio of 1.5 based on tunnel measurements, 2–5 in Guangzhou, and 6–15 in the manufacturing city of Dongguan. During KORUS-AQ the average T/B ratio over Seoul (calculated as the average ± 1σ of individual T/B values) was 7.6 ± 4.9 (median of 6.3), with ratios of 10–19 for toluene levels greater than 6 ppbv, suggesting a prominent influence of solvents on toluene (**Figure 7f**). By contrast the T/B ratio was 1.22 ± 0.05 in Lahore, Pakistan, a city heavily impacted by traffic emissions (*Barletta et al.*, 2017), and 1.05–1.27 in suburban areas of Beijing, also suggesting vehicle emissions (*Wang et al.*, 2012, 2016). While toluene is associated with both paint solvents and non-paint solvents (e.g., consumer products, printing), ethylbenzene and the xylenes are primarily associated with paint solvents (*Kwon et al.*, 2007; *Ou et al.*, 2015; *Wang et al.*, 2014). Consistent with this, ethylbenzene and the xylenes formed a tight correlating group in Seoul ($r^2$ = 0.85–0.99), with poorer correlation with toluene ($r^2$ = 0.53–0.75) and even poorer correlation with the vehicle exhaust tracers ethene and propene ($r^2$ = 0.23–0.42). Likewise, toluene showed poor correlation with ethene and propene ($r^2$ = 0.20–0.36). This suggests that paint solvents were a primary influence on ethylbenzene and the xylenes, and that toluene had mixed solvent impacts (both paint and non-paint).

The solvent influence on toluene in Seoul was further investigated by limited tunnel sampling during the blocking period on June 2, 2016 (15:12 local time) and June 5, 2016 (07:40 and 07:48), by filling WAS canisters and then analyzing them in the field using PTR-ToF-MS. The June 2 tunnel sample was taken within 15 mins of the DC-8 performing a missed approach over the Seoul Air Base during Flight 17, providing an excellent opportunity for direct comparison. Four WAS samples were collected aboard the DC-8 during the missed approach from 14:54–14:57 local time (alt. = 100–470 m), with an average T/B ratio of 8.4 ± 1.5 compared to 2.2 in the June 2 tunnel sample, clearly showing the additional impact of non-traffic sources on toluene in Seoul. A similar T/B ratio was measured in the Sangdo tunnel in Seoul in May 2000 (2.5 at the entrance and 2.2 in the middle of the tunnel; *Na et al.*, 2006).

Overall the analysis in Section 3.3.1 suggests that VOCs in Seoul during KORUS-AQ were impacted by biogenic sources, LPG, vehicle exhaust and solvents, with less prominent impact from gasoline evaporation, natural gas or biomass burning. Source apportionment was used to further investigate the sources of VOCs in Seoul, as discussed below.

#### 3.3.2. VOC source apportionment

Source apportionment was performed on the KORUS-AQ Seoul data ($n$ = 177) using EPA PMF Version 5.0 (Section 2.4). Multiple runs were performed using different numbers of gases and factors in order to select an optimal data set to use. VOCs were chosen based on their abundance (Section 3.2.1), their value as tracer gases (Section 3.3.1), and the ability of PMF to reproduce the observed mixing ratios. Sixteen VOCs were excluded because they had low mixing ratios and/or numerous values below detection (the butenes, $\alpha$- and $\beta$-pinene, styrene, and all $C_9$ aromatics). Methane and long-lived halocarbons (lifetime >6 mo) were not used, and the alkyl nitrates, which are secondary products in urban areas, also were not used. Other gases including shorter-lived halocarbons (e.g., $CHCl_3$, $C_2Cl_4$) were tested and rejected because the model did not reproduce the data well ($r^2$ of 0.31 to 0.50 for observed vs. predicted data). Likewise *n*-nonane, *n*-decane and the cycloalkanes were not used because, with the exception of cyclopentane, they included scaled residuals ($e_{ij}/u_{ij}$) outside the range of –3 to 3. Methanol was tested but not used because of a low signal-to-noise (S/N) ratio of 5.7.

Based on this data screening the designated PMF model run used 21 trace gases that were abundant in the SMA and represented tracers from a wide range of sources. This includes the biogenic tracer isoprene; combustion tracers CO and ethyne; vehicle exhaust tracers ethene and propene; natural gas tracer ethane; LPG tracers propane, *i*-butane and *n*-butane; gasoline evaporation tracers *i*-pentane and *n*-pentane; solvent tracers *n*-hexane, *n*-heptane, toluene, ethylbenzene, *m,p*-xylene, *o*-xylene, and the China tracer COS. Benzene, 2-methylpentane and 3-methylpentane were also included because of their abundance. *n*-Heptane was used despite having a data point with a scaled residual of 3.8 because of its value for distinguishing between paint and non-paint solvents (*Ou et al.*, 2015). Likewise propene, *i*-butane, *m,p*-xylene and *o*-xylene each had 1–2 data points with scaled residuals of 3.02–3.13, but were kept because of their value as tracers. All 21 compounds yielded a strong S/N ratio (9.9 for isoprene and *n*-heptane, and 10.0 for the remaining compounds) and the model reproduced the data well ($r^2$ of 0.78 to 0.96, where *n*-heptane had the weakest $r^2$ value and ethylbenzene had the strongest). The scaled residuals were normally distributed and were between –3 and 3 for most compounds as described above, indicating that they were well modeled (*Brown et al.*, 2007; *Wu et al.*, 2016). That is, PMF was able to model VOCs with a range of lifetimes and mixing ratios, including VOCs with log-normal distributions such as toluene.

The PMF model was run using between 3 and 6 factors, and each solution was assessed for how robust and reasonable it was. The 3-factor solution was muddled and failed to resolve a clear biogenic source. Indeed, isoprene had Q/Qexp = 5 in the 3-factor solution, whereas all species had Q/Qexp < 2 in the 4–6 factor solutions (from Section 2.4, Q/Qexp > 2 indicates that a species was not well modeled). Like the 3-factor solution, the 6-factor solution was also muddled, in its case because three factors split to create a new factor. For the 4-factor and

5-factor solutions, in general the 4-factor solution was more robust while the 5-factor solution was more reasonable. Both solutions are presented below, followed by a discussion of the limitations of the PMF analysis.

*Factor 1: Biogenic.* The 4-factor and 5-factor solutions both had a factor (called Factor 1) that was dominated by isoprene and was assigned a biogenic source (**Figure 9a, 9e**). This factor showed no rotational ambiguity for both the 4- and 5-factor solutions (no swap counts in the DISP diagnostics; *Brown et al.*, 2015). In reducing from 5 to 4 factors, the contribution of isoprene to Factor 1 remained similar (84% and 87%, respectively) whereas the contributions of non-biogenic VOCs increased by an average of 2.2 (Table S-3). For example, 7% of the combustion tracer ethyne was associated with Factor 1 with 5 factors, versus 13% with 4 factors. This suggests that the 5-factor solution is more reasonable for the biogenic source assignment, because non-biogenic VOCs contributed less to Factor 1 in the 5-factor solution. Factor 1 accounted for 13% and 7% of the source apportionment in the 4- and 5-factor solutions, respectively. Of the VOCs used in PMF, isoprene is the shortest-lived and the most sensitive to photochemistry (the isoprene lifetime is 3 hrs, followed by propene at 10 hrs; Table S-2). The sensitivity of the PMF results to photochemistry was investigated by increasing the amount of isoprene used in the PMF calculations. The biogenic contribution to the 4- and 5-factor solutions changed by +0.1 and +0.4%, respectively, with a 20% increase in isoprene, and by +1.7 and –0.6% with a 50% increase in isoprene. This suggests that potential impacts of photochemistry were relatively minor compared to other uncertainties in the PMF analysis.

*Factor 2: Long-range transport.* The 4- and 5-factor solutions both had a factor (Factor 2) that was characterized by the China tracer COS and longer-lived combustion tracers such as CO, ethyne and benzene, which together suggest long-range transport from China (**Figure 9b, 9f**). Similar to Factor 1, Factor 2 showed no rotational ambiguity for both solutions (no DISP swap counts). The contributions of the main VOC components were similar in both solutions (e.g., 67% for COS in both solutions; Table S-3), whereas the contributions of the minor components increased when reducing from 5 factors to 4. For example the contribution of toluene/ethylbenzene/xylenes (TEX) increased from 1–3% to 10–13% (Table S-3). That is, like the biogenic factor, switching from 5 to 4 factors caused some shorter-lived VOCs to contribute more to the long-range factor, suggesting that 5 factors is more reasonable. While Factor 2 includes tracers of incomplete combustion that could be associated with biomass burning (e.g., CO, ethyne), the Ministry of Environment Protection of the People's Republic of China reported very few wheat burning hotspots in China in May and June 2016 (*Y. Zhu, pers. comm.*, 2018; http://www.zhb.gov/cn/). Even though levels of the biomass burning tracer HCN were higher in air from China than in air from Seoul (Table S-3), the elevated HCN was likely associated with other fuel use such as domestic coal burning (*Crounse et al.*, 2009; *Du et al.*, 2016) given the insignificant biomass burning in the region. Factor 2 accounted for 24% and 20% of the

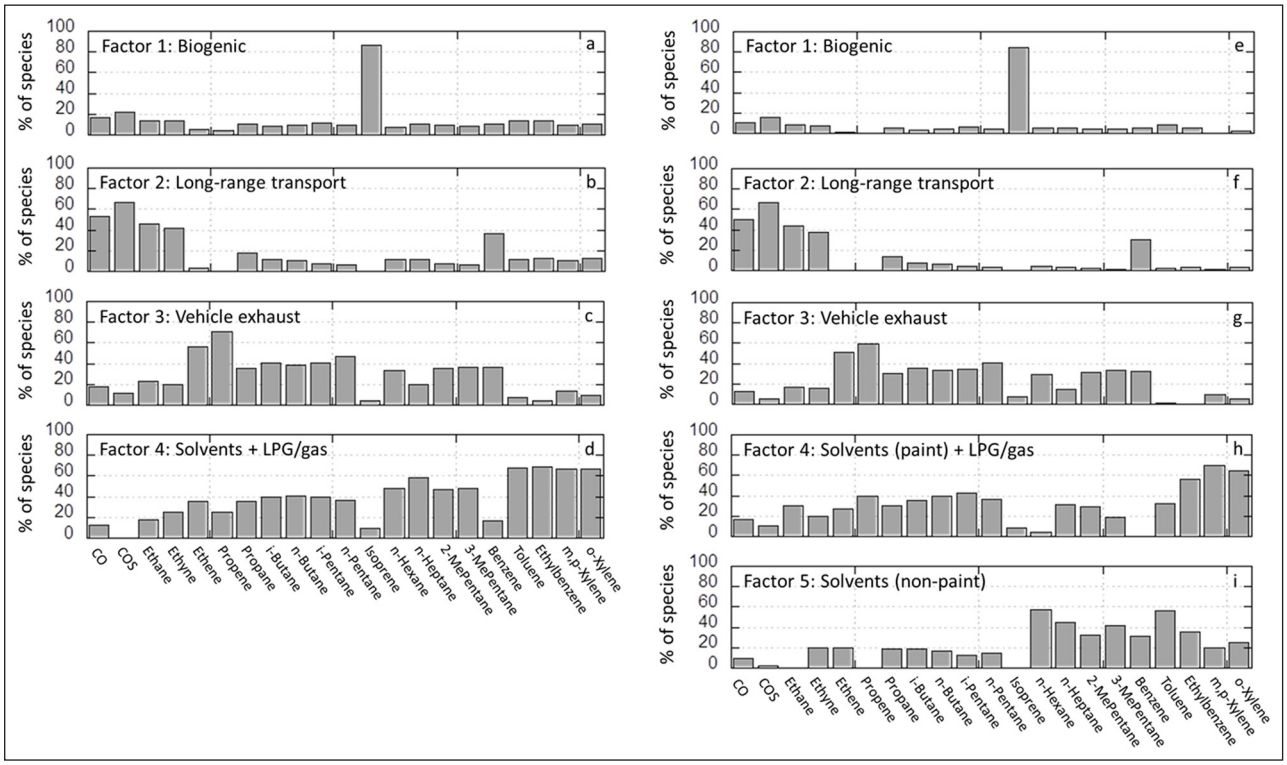


**Figure 9: Source apportionment results for selected VOCs measured over Seoul during KORUS-AQ.** The PMF analysis uses air samples collected at low altitude (<0.5 km; $n$ = 177). Results are shown for **(a–d)** a four factor solution and **(e–i)** a five factor solution. See text for details. DOI: https://doi.org/10.1525/elementa.434.f9

source apportionment in the 4-factor and 5-factor solutions, respectively.

*Factor 3: Vehicle exhaust.* The remaining factors in the 4- and 5-factor solutions were associated with traffic and solvents. Both solutions had a factor (Factor 3) with highest loadings of the vehicle exhaust tracers ethene and propene, as well as other compounds associated with vehicle exhaust such as benzene and light alkanes (**Figure 9c, 9g**). Unlike Factors 1 and 2, Factor 3 had some rotational ambiguity in the 5-factor solution (6 DISP swap counts), meaning that caution should be used when interpreting the 5-factor solution. Factor 3 accounted for 57% and 52% of the ethene and 71% and 60% of the propene in the 4- and 5-factor solutions, respectively (Table S-3). The prominence of ethene and propene suggests that Factor 3 captured Seoul's diesel emissions (Section 3.3.1). The combustion tracer ethyne did not associate especially strongly with Factor 3 (20% and 15% in the 4- and 5-factor solutions, respectively), though this has been previously observed in Hong Kong where ethyne emissions from gasoline-fueled cars were negligible and caution was suggested when using ethyne as a tracer of vehicle emissions (*Guo et al.*, 2011a). Even though aromatics are emitted by vehicle exhaust, the aromatics except benzene had a relatively weak contribution to Factor 3 because solvents were a much stronger influence than traffic on the TEX aromatics in Seoul (Section 3.3.1; also see below). The combustion tracer CO also had a relatively small association with this factor (18% and 12% in the 4- and 5-factor solutions, respectively), and instead CO was most associated with Factor 2, the long-range transport source (53% and 51%, respectively; Table S-3). This is broadly consistent with analysis by Halliday et al. (2019), who found that $\Delta CO/\Delta CO_2$ showed regional differences during KORUS-AQ, with a lower ratio (~1%) over Seoul reflecting efficient combustion, and a higher ratio (2–4%) at higher altitudes and over the West Sea reflecting less efficient combustion in air arriving from China. The vehicle exhaust source accounted for 27% and 21% of the source apportionment in the 4- and 5-factor solutions, respectively.

*Factor 4: Mixed source.* The fourth factor (Factor 4) was more complex than the first three factors and was different for the 4-factor and 5-factor solutions. The 4-factor solution had highest loadings of TEX compounds (67–69%), followed by $C_3$–$C_7$ alkanes and $C_2$–$C_3$ alkenes (**Figure 9d**; Table S-3). That is, the 4-factor solution showed a mix of VOCs that can be related to solvents, traffic and cleaner fuels. In broad terms, this factor split into two factors in the 5-factor solution (Factors 4 and 5). While Factor 4 of the 5-factor solution showed less rotational ambiguity (1 DISP swap) than Factor 5 (6 DISP swaps), both factors are interpreted with caution. Factor 4 of the 5-factor solution retained most of the xylenes (65–70%), ethylbenzene (56%), $C_3$–$C_5$ alkanes and $C_2$–$C_3$ alkenes (**Figure 9h**; Table S-3), and this factor appears to be a mixed source. The strong contributions from ethylbenzene and the xylenes suggest impact from paint solvents, as discussed in Section 3.3.1. The presence of traffic tracers ethene and propene together with light alkanes suggests contributions from gasoline and LPG fuels. The ratio of *i*-pentane/*n*-pentane is higher in this factor (1.7) than in the other traffic and solvent factors (1.20–1.25), suggesting that gasoline evaporation may contribute to this factor even if its overall impact in Seoul is relatively small (Section 3.3.1). Therefore the alkenes and alkanes associated with Factor 4 are consistent with cleaner fuels and a mix of combustive and evaporative emissions. This mixed fuel and solvent source accounted for 36% and 32% of the source apportionment in the 4- and 5-factor solutions, respectively.

*Factor 5: Solvents (non-paint).* Factor 5 had highest loadings of toluene (57%), *n*-hexane (57%) and *n*-heptane (45%), followed by methylpentanes, ethylbenzene and the xylenes (**Figure 9i**; Table S-3). In other words, consistent with the correlation analysis is Section 3.3.1, it is notable that toluene associates more strongly with a different factor than ethylbenzene and the xylenes, implying different source influences for individual TEX species. Previous work in Asia has found that the printing industry is toluene-rich (*Tang et al.*, 2014) and that *n*-hexane and *n*-heptane are also tracers of the consumer products and printing industry, for example disinfectants, air fresheners, furniture polishes, sealants and offset printing (*Kwon et al.*, 2007; *Ou et al.*, 2015; *Shen et al.*, 2018). As noted in Section 3.3.1, though aromatics can be emitted from vehicle exhaust, the high T/B ratio and poor correlation of toluene with traffic tracers both suggest a predominant impact from solvents rather than vehicle exhaust on toluene in Seoul. While recognizing that there can be significant regional differences in VOC source emission signatures (*Yuan et al.* 2010; *Zheng et al.*, 2013), Factor 5 is consistent with non-paint solvents such as consumer products and printing. The association of methylpentanes with this factor suggests some solvent influence on methylpentanes in Seoul in addition to traffic. Factor 5 accounted for 20% of the source apportionment.

#### 3.3.3. Discussion of VOC sources and comparison with emission inventory

A combination of complementary techniques was used to investigate the most likely sources of VOCs in Seoul. VOC tracers, correlations and ratios identified contributions from vehicle exhaust, solvents, LPG and biogenic sources, and ruled out major impacts from gasoline evaporation, natural gas and biomass burning. Source apportionment identified vehicle exhaust, solvents, cleaner fuels such as LPG, biogenic and long-range transport sources, with a separation of paint and non-paint solvents depending on how many factors were used. While PMF can quantify the contributions of each source to the measured VOCs, these quantitative results should be interpreted with caution. On the one hand, although the 4-factor solution was more robust than 5-factors, it was not necessarily more reasonable because several VOCs became mis-assigned. On the other hand, while the 5-factor solution was able to separate paint and non-paint solvents, which is useful for informing policy, it showed some rotational

ambiguity. Because the separation of paint and non-paint solvents was also evident in simple correlation analysis, and because the 5-factor solution was more reasonable for the biogenic and long-range source factors, we suggest that the 5-factor solution can be used with appropriate uncertainty considerations. The average difference between the 4 and 5-factor solutions was about 5% (Table S-3), and this is likely the minimum uncertainty for interpreting the PMF results. Therefore, bearing in mind this uncertainty, the measured VOCs in Seoul are represented by biogenic sources (7%), long-range transport (20%), vehicle exhaust (21%), non-paint solvents (20%) and a mix of paint solvents and cleaner fuels (32%).

While recognizing that the mixed source provides a range of uncertainty, the 5-factor PMF results suggest roughly equal contributions of vehicular emissions (21–53%) and solvents (20–52%) to VOC levels over Seoul, with a maximum solvent contribution of 52% for the mix of VOCs that was used (though this value is unlikely as it would require fuel tracers to be accounted for by solvents). These PMF results yield relatively less solvent impact on total VOCs than the KORUSv5 EI for Seoul (82% solvents, 15% mobile). However it is important to recognize additional uncertainties in this comparison. For example the KORUS-AQ source apportionment is based on CO and 20 VOCs using focused measurements during springtime, while the KORUSv5 EI is based on 30 VOC groups that were speciated from annual NMVOC estimations in the CAPSS inventory. The uncertainties in the chemical speciation process, which converts total NMVOCs to speciated model-ready data, and in the temporal allocation process, which converts the 2015 annual estimation to monthly values, could be other sources of uncertainty. Overall, vehicle emission control measures and fuel substitution strategies are well established in South Korea, and the PMF results and KORUSv5 EI both point to solvents as a major source of reactive VOCs that could be further pursued for VOC emission reductions.

### *3.4. Recommendations for VOC reductions*

Using multiple data analysis techniques based on 82 VOCs measured in whole air samples and selected OVOCs measured using PTR-ToF-MS, this study has identified light alkenes (isoprene, ethene, propene), $C_7$–$C_8$ aromatics (toluene, xylenes and ethylbenzene) and methanol as major precursors to ozone formation in Seoul. The aromatics also contribute to SOA formation (*Nault et al.*, 2018). Ozone formation in Seoul is more sensitive to VOCs than $NO_x$ (*H. Kim et al.*, 2018b; *S. Kim et al.*, 2018), similar to many cities in Asia (*Guo et al.*, 2017). Because VOC reductions in South Korea have been slower than $NO_x$ and because air pollution in Seoul may worsen under increasing ratios of VOCs/$NO_x$ (*Kim and Lee*, 2018), aromatics and alkenes are attractive targets for VOC emission reduction strategies. Vehicle exhaust was identified as the main source of ethene and propene emissions, and solvents were the main sources of aromatics, primarily paint solvents for ethylbenzene and the xylenes, and non-paint solvents (e.g., consumer and printing products) for toluene. In other words, aromatic (TEX) reductions can best be achieved by targeting solvents rather than traffic, with a focus on multiple solvent products including both paint and non-paint solvents. This step would complement and expand on existing strategies to limit VOC content in paints, in addition to long-established policies in South Korea to limit emissions from vehicle exhaust.

A similar strategy has been successfully applied in Hong Kong, a city where toluene used to be the most abundant VOC and where policies that regulate the VOC content in solvent products have led to a decline in toluene levels (*Guo et al.*, 2006; *Lyu et al.*, 2017). Specifically, the Hong Kong government prescribed VOC content limits for 172 types of regulated products including architectural paints, printing inks, consumer products, vehicle refinishing coatings, vessel and pleasure craft coatings, adhesives and sealants, fountain solutions, and printing machine cleansing agents (*P.K.K. Louie, pers. comm.*, 2018).

## 4. Conclusions

The 2016 KORUS-AQ study provided a focused opportunity to study the characteristics, sources and ozone-forming potential of VOCs in Seoul and its surrounding regions during spring. Based on VOC measurements in 2554 whole air samples, distinct VOC signatures were characterized for major emission regions, including the Seoul region and the Daesan petrochemical facility in northwest Korea, the Busan region of southeast Korea, and air originating from China during periods of dynamic transport. In addition to methanol, formaldehyde, ethane and propane, Seoul air was particularly toluene-rich and Daesan air was rich in ethene and benzene. Levels of $CCl_4$ and H-2402 stood out in Busan. Recommended tracers of air from China during KORUS-AQ include COS,1,2-dichloroethane, CFC-113, CFC-114 and $CCl_4$. While Halon 1211 used to be a good tracer of air from China, this is no longer the case because its production in China has been phased out. Although CFC-11 was elevated in air from China, it was surprisingly more enriched in air from Seoul including during stagnant periods.

Low altitude air samples collected over Seoul were analyzed using a combination of techniques. Isoprene, toluene, xylenes and ethene were strong individual contributors to OH reactivity in Seoul, similar to results from major urban areas of China. While methanol was also a strong contributor to OH reactivity, photochemical box modeling showed a lower impact of methanol on ozone formation in Seoul, which is attributed to the model's more realistic handling of radical chemistry. Both the OH reactivity calculations and photochemical box modeling agreed that ozone production in Seoul is most sensitive to aromatics, followed by isoprene and anthropogenic alkenes. These results highlight the importance of source apportionment studies and other techniques that can identify specific source sectors for VOCs, particularly for individual aromatics. Correlations, ratio analysis and source apportionment all pointed to stronger influence from solvents than traffic on the reactive TEX aromatics. Separation of the solvents source provided valuable information to guide strategies for reducing emissions of aromatics that are implicated in $O_3$ and SOA formation.

Specifically, ethylbenzene and the xylenes were more associated with paint solvents and toluene with non-paint solvents. Therefore, in addition to current programs that limit VOC emissions from vehicles and the VOC content in paints, this work suggests that content limits on additional volatile chemical products, for example consumer products and printing agents, could help achieve the goal of reducing aromatic levels in Seoul, especially toluene, as part of ongoing efforts to improve air quality.

## Data Accessibility Statement

All observational data from the KORUS-AQ mission, including the WAS VOC data, are archived at: https://www-air.larc.nasa.gov/cgi-bin/ArcView/korusaq.

## Supplemental file

The supplemental file for this article can be found as follows:

- **Supplemental Material.** Characterization, Sources and Reactivity of Volatile Organic Compounds (VOCs) in Seoul and Surrounding Regions during KORUS-AQ. DOI: https://doi.org/10.1525/elementa.434.s1

## Acknowledgements

The KORUS-AQ mission was jointly funded by NASA and the Korean National Institute of Environmental Research (NIER). We gratefully acknowledge the KORUS-AQ crew and science team, and the technicians and staff at UC-Irvine who supported the WAS effort (Barbara Chisholm, Gloria Liu Weitz, Brent Love, Nick Vizenor, Rafe Day). The $NO_y$ and $O_3$ data were provided courtesy of Andrew Weinheimer and Denise Montzka (NCAR), and John Crounse provided HCN data. The PTR-ToF-MS measurements were supported by the Austrian Federal Ministry for Transport, Innovation and Technology (bmvit) through the Austrian Space Applications Programme (ASAP) of the Austrian Research Promotion Agency (FFG). The PTR-ToF-MS instrument team (P. Eichler, L. Kaser, M. Müller) is acknowledged for their support in the field and during the mission preparation phase, and Ionicon Analytik is acknowledged for instrumental support. We also thank Daniel Bon (Colorado Dept. of Public Health & Environment) for helpful discussions on PMF, Hannah Halliday (NASA Langley) and Meehye Lee (Korea University) for helpful discussions on regional source influences, Saewung Kim (UCI) for coordination during the MAPS-2015 campaign, and Yanhong Zhu (Jinan University) for providing wheat count hotspots during the KORUS-AQ timeframe. We thank the UC White Mountain Research Center for use of the Crooked Creek Station for gathering air samples for use as working standards. Finally we thank numerous colleagues for valuable discussions and feedback on the interpretation of the source apportionment results.

## Competing interests

The authors have no competing interests to declare.

## Author contributions

IJS interpreted the data and wrote the manuscript. DRB oversaw the WAS contribution to KORUS-AQ and performed data analysis and interpretation. NJB oversaw WAS field operations, and NJB, SCH and LTF acquired WAS data. SM oversaw WAS laboratory operations and performed data analysis. BB oversaw WAS data management. JHC and JRS performed photochemical box modeling calculations and data interpretation. GSD and SEP provided CO and $CH_4$ measurements. HG, DW and IZ supported the PMF analysis. DAP oversaw the meteorological analysis. AW and TM performed PTR-ToF-MS analysis. JHW, JK and YK oversaw the KORUSv5 emission inventory and provided data for the paper. AF led the $CH_2O$ analysis. LKE, JB and BG provided CAM-chem model simulations. CK provided the FLEXPART back trajectories. POW and MJK provided HCN data. All co-authors revised the manuscript and approved the submitted version for publication.

## References

**Abeleira, A, Pollack, IB, Sive, B, Zhou, Y, Fishcer, EV** and **Farmer, DK.** 2017. Source characterization of volatile organic compounds in the Colorado Northern Front Range Metropolitan Area during spring and summer 2015. *J. Geophys. Res. Atmos.* **122**: 3595–3613. DOI: https://doi.org/10.1002/2016JD026227

**Ainsworth, EA, Yendrek, CR, Sitch, S, Collins, WJ** and **Emberson, LD.** 2012. The effects of tropospheric ozone on net primary productivity and implications for climate change. *Annu. Rev. Plant Biol.* **63**: 637–661. DOI: https://doi.org/10.1146/annurev-arplant-042110-103829

**Akagi, SK, Yokelson, RJ, Wiedinmyer, C, Alvarado, MJ, Reid, JS, Karl, T, Crounse, JD** and **Wennberg, PO.** 2011. Emission factors for open and domestic biomass burning for use in atmospheric models. *Atmos. Chem. Phys.* **11**: 4039–4072. DOI: https://doi.org/10.5194/acp-11-4039-2011

**Al-Saadi, J, Carmichael, G, Crawford, J, Emmons, L, Kim, S, Song, C-K, Chang, L-S, Lee, G, Kim, J** and **Park, R.** 2015. *NASA Contributions to KORUS-AQ: An International Cooperative Air Quality Field Study in Korea, NASA*. https://www-air.larc.nasa.gov/missions/korus-aq/docs/White_paper_NASA_KORUS-AQ.pdf (accessed May 2019).

**Atkinson, R** and **Arey, J.** 2003. Atmospheric degradation of volatile organic compounds. *Chem. Rev.* **103**: 4605–4638. DOI: https://doi.org/10.1021/cr0206420

**Atkinson, R, Baulch, DL, Cox, RA, Crowley, JN, Hampson, RF, Hynes, RG, Jenkin, ME, Rossi, MJ** and **Troe, J.** 2004. Evaluated kinetic and photochemical data for atmospheric chemistry: Volume I – gas phase reactions of $O_x$, $HO_x$, $NO_x$ and $SO_x$ species. *Atmos. Chem. Phys.* **4**: 1461–1738. DOI: https://doi.org/10.5194/acp-4-1461-2004

**Atkinson, R, Baulch, DL, Cox, RA, Crowley, JN, Hampson, RF, Hynes, RG, Jenkin, ME, Rossi, MJ** and **Troe, J.** 2006. Evaluated kinetic and photochemical data for atmospheric chemistry: Volume II – gas phase reactions of organic species. *Atmos. Chem. Phys.* **6**: 3625–4055. DOI: https://doi.org/10.5194/acp-6-3625-2006

**Atkinson, R, Baulch, DL, Cox, RA, Crowley, JN, Hampson, RF, Hynes, RG, Jenkin, ME, Rossi, MJ, Troe, J** and **Wallington, TJ.** 2008. Evaluated kinetic and photochemical data for atmospheric chemistry: Volume IV – gas phase reactions of organic halogen species. *Atmos. Chem. Phys.* **8**: 4141–4496. DOI: https://doi.org/10.5194/acp-8-4141-2008

**Baker, AK, Beyersdorf, AJ, Doezema, LA, Katzenstein, A, Meinardi, S, Simpson, IJ, Blake, DR** and **Rowland, FS.** 2008. Measurements of nonmethane hydrocarbons in 28 United States cities. *Atmos. Environ.* **42**: 170–182. DOI: https://doi.org/10.1016/j.atmosenv.2007.09.007

**Barletta, B, Meinardi, S, Rowland, FS, Chan, C-Y, Wang, X, Zou, S, Chan, LY** and **Blake, DR.** 2005. Volatile organic compounds in 43 Chinese cities. *Atmos. Environ.* **39**: 5979–5990. DOI: https://doi.org/10.1016/j.atmosenv.2005.06.029

**Barletta, B, Meinardi, S, Simpson, IJ, Atlas, EL, Beyersdorf, AJ, Baker, AK, Blake, NJ, Yang, M, Midyett, JR, Novak, BJ, McKeachie, RJ, Fuelberg, HE, Sachse, GW, Avery, MA, Campos, T, Weinheimer, AJ, Rowland, FS** and **Blake, DR.** 2009. Characterization of volatile organic compounds (VOCs) in Asian and north American pollution plumes during INTEX-B: identification of specific Chinese air mass tracers. *Atmos. Chem. Phys.* **9**: 5371–5388. DOI: https://doi.org/10.5194/acp-9-5371-2009

**Barletta, B, Simpson, IJ, Blake, NJ, Meinardi, S, Emmons, LK, Aburizaiza, OS, Siddique, A, Zeb, J, Yu, LE, Khwaja, HA, Farrukh, MA** and **Blake, DR.** 2017. Characterization of carbon monoxide, methane and nonmethane hydrocarbons in emerging cities of Saudi Arabia and Pakistan and in Singapore. *J. Atmos. Chem.* **74**(1): 87–113. DOI: https://doi.org/10.1007/s10874-016-9343-7

**Blake, NJ, Blake, DR, Simpson, IJ, Meinardi, S, Swanson, AL, Lopez, JP, Katzenstein, AS, Barletta, B, Shirai, T, Atlas, E, Sachse, G, Avery, M, Vay, S, Fuelberg, HE, Kiley, CM, Kita, K** and **Rowland, FS.** 2003. NMHCs and halocarbons in Asian continental outflow during the Transport and Chemical Evolution over the Pacific (TRACE-P) field campaign: Comparison with PEM-West B. *J. Geophys. Res.* **108**(D20): 8806. DOI: https://doi.org/10.1029/2002JD003367

**Blake, NJ, Streets, DG, Woo, J-H, Simpson, IJ, Green, J, Meinardi, S, Kita, K, Atlas, E, Fuelberg, HE, Sachse, G, Avery, MA, Vay, SA, Talbot, RW, Dibb, JE, Bandy, AR, Thornton, DC, Rowland, FS** and **Blake, DR.** 2004. Carbonyl sulfide and carbon disulfide: Large-scale distributions over the western Pacific and emissions from Asia during TRACE-P. *J. Geophys. Res.* **109**: D15S05. DOI: https://doi.org/10.1029/2003JD004259

**Bon, DM, Ulbrich, IM, de Gouw, JA, Warneke, C, Kuster, WC, Alexander, ML, Baker, A, Beyersdorf, AJ, Blake, D, Fall, R, Jimenez, JL, Herndon, SC, Huey, LG, Knighton, WB, Ortega, J, Springston, S** and **Vargas, O.** 2011. Measurements of volatile organic compounds at a suburban ground site (T1) in Mexico City during the MILAGRO 2006 campaign: measurement comparison, emission ratios, and source attribution. *Atmos. Chem. Phys.* **11**: 2399–2421. DOI: https://doi.org/10.5194/acp-11-2399-2011

**Borbon, A, Fontaine, H, Veillerot, M, Locoge, N, Galloo, JC** and **Guillermo, R.** 2001. An investigation into the traffic-related fraction of isoprene at an urban location. *Atmos. Environ.* **35**: 3747–3760. DOI: https://doi.org/10.1016/S1352-2310(01)00170-4

**Brown, SG, Eberly, S, Paatero, P** and **Norris, GA.** 2015. Methods for estimating uncertainty in PMF solutions: Examples with ambient air and water quality data and guidance on reporting PMF results. *Sci. Total Environ.* **518–519**: 626–635. DOI: https://doi.org/10.1016/j.scitotenv.2015.01.022

**Brown, SG, Frankel, A** and **Hafner, HR.** 2007. Source apportionment of VOCs in the Los Angeles area using positive matrix factorization. *Atmos. Environ.* **41**: 227–237. DOI: https://doi.org/10.1016/j.atmosenv.2006.08.021

**Cai, C, Geng, F, Tie, X, Yu, Q** and **An, J.** 2010. Characteristics and source apportionment of VOCs measured in Shanghai, China. *Atmos. Environ.* **44**: 5005–5014. DOI: https://doi.org/10.1016/j.atmosenv.2010.07.059

**Cao, X, Yao, Z, Shen, X, Ye, Y** and **Jiang, X.** 2016. On-road emission characteristics of VOCs from light-duty gasoline vehicles in Beijing, China. *Atmos. Environ.* **124**: 146–155. DOI: https://doi.org/10.1016/j.atmosenv.2015.06.019

**Campbell, JE, Whelan, ME, Seibt, U, Smith, SJ, Berry, JA** and **Hilton, TW.** 2015. Atmospheric carbonyl sulfide sources from anthropogenic activity: Implications for carbon cycle constraints. *Geophys. Res. Lett.* **42**: 3004–3010. DOI: https://doi.org/10.1002/2015GL063445

**Carter, WPL.** May 2000. *Documentation of the SAPRC-99 Chemical Mechanism for VOC Reactivity Assessment*, 92–329 and 95–308. Report to the California Air Resources Board, Contracts. Available at http://www.cert.ucr.edu/~carter/reactdat.htm.

**Chang, KL, Petropavlovskikh, I, Cooper, OR, Schultz, MG** and **Wang, T.** 2017. Regional trend analysis of surface ozone observations from monitoring networks in eastern North America, Europe and East Asia. *Elem. Sci. Anth.* **5**: 50. DOI: https://doi.org/10.1525/elementa.243

**Colman, JJ, Swanson, AL, Meinardi, S, Sive, BC, Blake, DR** and **Rowland, FS.** 2001. Description of the analysis of a wide range of volatile organic compounds in whole air samples collected during PEM-Tropics A and B. *Anal. Chem.* **73**: 3723–3731. DOI: https://doi.org/10.1021/ac010027g

**Crawford, JH, Ahn, J-Y, Al-Saadi, J, Chang, L, Emmons, L, Kim, J, Lee, G, Park, J-H, Park, R, Woo, J-H** and **Lefer, B.** 2020. The Korea-United States Air Quality (KORUS-AQ) Field Study. *Elem. Sci. Anth.* this Special Feature, to be submitted.

**Crounse, JD, DeCarlo, PF, Blake, DR, Emmons, LK, Campos, TL, Apel, EC, Clarke, AD, Weinheimer, AJ, McCabe, DC, Yokelson, RJ, Jimenez, JL** and **Wennberg, PO.** 2009. Biomass burning and urban air pollution over the Central Mexican Plateau. *Atmos. Chem. Phys.* **9**: 4929–4944. DOI: https://doi.org/10.5194/acp-9-4929-2009

**Dai, P, Ge, Y, Lin, Y, Su, S** and **Liang, B.** 2013. Investigation on characteristics of exhaust and evaporative emissions from passenger cars fueled with gasoline/methanol blends. *Fuel* **113**: 10–16. DOI: https://doi.org/10.1016/j.fuel.2013.05.038

**Du, Q, Zhang, C, Mu, Y, Cheng, Y, Zhang, Y, Liu, C, Song, M, Tian, D, Liu, P, Liu, J, Xue, C** and **Ye, C.** 2016. An important missing source of atmospheric carbonyl sulfide: Domestic coal combustion. *Geophys. Res. Lett.* **43**: 8720–8727. DOI: https://doi.org/10.1002/2016GL070075

**Energy Smart Communities Initiative (ESCI) Knowledge Sharing Platform.** 2018. *Intelligent transportation systems.* http://esci-ksp.org/project/100-cng-fueled-buses-in-seoul/ (accessed May 2019).

**Fleming, ZL, Doherty, RM, von Schneidemesser, E, Malley, CS, Cooper, OR, Pinto, JP, Colette, A, Xu, X, Simpson, D, Schultz, MG, Lefohn, AS, Hamad, S, Moolla, R, Solberg, S** and **Feng, Z.** 2018. Tropospheric Ozone Assessment Report: Present-day ozone distribution and trends relevant to human health. *Elem. Sci. Anth.* **6**: 12. DOI: https://doi.org/10.1525/elementa.273

**Fraser, MP, Cass, GR** and **Simoneit, BRT.** 1998. Gas-phase and particle-phase organic compounds emitted from motor vehicle traffic in a Los Angeles roadway tunnel. *Environ. Sci. Technol.* **32**(4): 2051–2060. DOI: https://doi.org/10.1021/es970916e

**Fraser, PJ, Omarm, DE, Reeves, CE, Penkett, SA** and **McCulloch, A.** 1999. Southern Hemispheric halon trends (1978–1998) and global halon emissions. *J. Geophys. Res.* **104**(D13): 15,985–15,999. DOI: https://doi.org/10.1029/1999JD900113

**Fried, A, Walega, J, Weibring, P, Richter, D, Simpson, IJ, Blake, DR, Blake, NJ, Meinardi, S, Barletta, B, Hughes, SC, Crawford, JH, Diskin, G, Barrick, J, Hair, J, Wisthaler, A, Mikoviny, T, Woo, J-H, Kim, J, Min, K-E, Jeong, S, Wennberg, PO, Kim, M, Crounse, JD, Teng, AP, Benett, R, Huey, G, Weinheimer, A, Knote, C, Kim, JH, Kim, S-J** and **Brune, W.** 2020. Airborne formaldehyde and VOC measurements over the Daesan petrochemical complex on Korea's northwest coast during the KORUS-AQ study: Estimation of emission fluxes and effects on air quality. *Elem. Sci. Anth.*, to be submitted.

**Gao, J, Zhang, J, Li, H, Li, L, Xu, L, Zhang, Y, Wang, Z, Wang, X, Zhang, W, Chen, Y, Cheng, X, Zhang, H, Peng, L, Chai, F** and **Wei, Y.** 2018. Comparative study of volatile organic compounds in ambient air using observed mixing ratios and initial mixing ratios taking chemical loss into account – A case study in a typical urban area in Beijing. *Sci. Total Environ.* **628–629**: 791–804. DOI: https://doi.org/10.1016/j.scitotenv.2018.01.175

**Gilman, JB, Lerner, BM, Kuster, WC** and **de Gouw, JA.** 2013. Source signatures of volatile organic compunds from oil and natural gas operations in northeastern Colorado. *Environ. Sci. Technol.* **47**(3): 1297–1305. DOI: https://doi.org/10.1021/es304119a

**Guenther, AB, Jiang, X, Heald, CL, Sakulyanontvittaya, T, Duhl, T, Emmons, LK** and **Wang, X.** 2012. The Model of Emissions of Gases and Aerosols from Nature version 2.1 (MEGAN2.1): an extended and updated framework for modeling biogenic emissions. *Geosci. Model. Dev.* **5**: 1471–1492. DOI: https://doi.org/10.5194/gmd-5-1471-2012

**Guo, H, Cheng, HR, Ling, ZH, Louie, PKK** and **Ayoko, GA.** 2011b. Which emission sources are responsible for the volatile organic compounds in the atmosphere of Pearl River Delta? *J. Hazard. Mat.* **188**: 116–124. DOI: https://doi.org/10.1016/j.jhazmat.2011.01.081

**Guo, H, Ling, ZH, Cheng, HR, Simpson, IJ, Lyu, XP, Wang, XM, Shao, M, Lu, HX Ayoko, G, Zhang, YL, Saunders, SM, Lam, SHM, Wang, JL** and **Blake, DR.** 2017. Tropospheric volatile organic compounds in China. *Sci. Total Environ.* **574**: 1021–1043. DOI: https://doi.org/10.1016/j.scitotenv.2016.09.116

**Guo, H, Wang, T, Blake, DR, Simpson, IJ, Kwok, YH** and **Li, YS.** 2006. Regional and local contributions to ambient non-methane volatile organic compounds at a polluted rural/coastal site in Pearl River Delta, China. *Atmos. Environ.* **40**: 2345–2359. DOI: https://doi.org/10.1016/j.atmosenv.2005.12.011

**Guo, H, Zou, SC, Tsai, WY, Chan, LY** and **Blake, DR.** 2011a. Emission characteristics of nonmethane hydrocarbons from private cars and taxis at different driving speeds in Hong Kong. *Atmos. Environ.* **45**: 2711–2721. DOI: https://doi.org/10.1016/j.atmosenv.2011.02.053

**Halliday, HS, DiGangi, JP, Choi, Y, Diskin, GS, Pusede, SE, Rana, M, Nowak, JB, Knote, C, Ren, X, He, H, Dickerson, RR** and **Li, Z.** 2019. Using short-term $CO/CO_2$ ratios to assess air mass differences over the Korean Peninsula during KORUS-AQ. *J. Geophys. Res.* In press. DOI: https://doi.org/10.1029/2018JD029697

**Hopke, PK.** 2016. Review of receptor modeling methods for source apportionment. *J. Air Waste Manage. Assoc.* **66**(3): 237–259. DOI: https://doi.org/10.1080/10962247.2016.1140693

**Hornbrook, RS, Blake, DR, Diskin, GS, Fried, A, Fuelberg, HE, Meinardi, S, Mikoviny, T, Richter, D, Sachse, GW, Vay, SA, Walega, J, Weibring, P, Weinheimer, AJ, Wiedinmyer, C, Wisthaler, A, Hills, A, Riemer, DD** and **Apel, EC.** 2011. *Atmos. Chem. Phys.* **11**: 11,103–11,130. DOI: https://doi.org/10.5194/acp-11-11103-2011

**International Agency for Research on Cancer (IARC).** 2013. *Outdoor Air Pollution as a Leading Environmental Cause of Cancer Deaths.* Lyon, France: World Health Organization. http://iarc.fr/en/media-centre/pr/2013/pdfs/pr221_E.pdf.

**Jacob, DJ, Field, BD, Li, Q, Blake, DR, de Gouw, J, Warneke, C, Hansel, A, Wisthaler, A, Singh, HB** and **Guenther, A.** 2005. Global budget of methanol: Constraints from atmospheric observations. *J. Geophys. Res.* **110**: D08303. DOI: https://doi.org/10.1029/2004JD005172

**Kado, N, Okamoto, RA, Kuzmicky, PA, Kobayashi, R, Ayala, A, Gebel, ME, Rieger, PL, Maddox, C** and **Zafonte, L.** 2005. Emissions of toxic pollutants from compressed natural gas and low sulfur diesel-fueled heavy-duty transit buses tested over multiple driving cycles. *Environ. Sci. Technol.* **39**: 7638–7649. DOI: https://doi.org/10.1021/es0491127

**Khan, MAH, Schlich, B-L, Jenkin, ME, Shallcross, BMA, Moseley, K, Walker, C, Morris, WC, Derwent, RG, Percival, CJ** and **Shallcross, D.** 2018. A two-decade anthropogenic and biogenic isoprene emissions study in a London urban background and a London urban traffic site. *Atmosphere* **9**: 387. DOI: https://doi.org/10.3390/atmos9100387

**Kille, N, Chiu, R, Frey, M, Hase, F, Sha, MK, Blumenstock, T, Hannigan, JW, Orphal, J, Bon, D** and **Volkamer, R.** 2019. Separation of methane emissions from agricultural and natural gas sources in the Colorado Front Range. *Geophys. Res. Lett.* **46**: 3990–3998. DOI: https://doi.org/10.1029/2019GL082132

**Kim, H, Choi, W-C, Rhee, H-J, Suh, I, Lee, M, Blake, DR, Kim, S, Jung, J, Lee, G, Kim, D-S, Park, S-M, Ahn, J** and **Lee, SD.** 2018b. Meteorological and chemical factors controlling ozone formation in Seoul during MAPS-Seoul 2015. *Aerosol Air Qual. Res.* **18**: 2274–2286. DOI: https://doi.org/10.4209/aaqr.2017.11.0445

**Kim, S, Jeong, D, Sanchez, D, Wang, M, Seco, R, Blake, D, Meinardi, S, Barletta, B, Hughes, S, Jung, J, Kim, D, Lee, G, Lee, M, Ahn, J, Lee, S-D, Cho, G, Sung, M-Y, Lee, Y-L** and **Park, R.** 2018. The controlling factors of photochemical ozone production in Seoul, South Korea. *Aerosol Air Qual. Res.* **18**: 2253–2261. DOI: https://doi.org/10.4209/aaqr.2017.11.0452

**Kim, S, Sanchez, D, Wang, M, Seco, R, Jeong, D, Hughes, S, Barletta, B, Blake, DR, Jung, J, Kim, D, Lee, G, Lee, M, Ahn, J, Lee, S-D, Cho, G, Sung, M-Y, Lee, Y-H, Kim, DB, Kim, Y, Woo, J-H, Jo, D, Park, R, Park, J-H, Hong, Y-D** and **Hong, J-H.** 2016. OH reactivity in urban and suburban regions in Seoul, South Korea – an East Asian megacity in a rapid transition. *Faraday Discuss.* **189**: 231–251. DOI: https://doi.org/10.1039/C5FD00230C

**Kim, H, Zhang, Q** and **Heo, J.** 2018a. Influence of intense secondary aerosol formation and long-range transport on aerosol chemistry and properties in the Seoul Metropolitan Area during spring time: results from KORUS-AQ. *Atmos. Chem. Phys.* **18**: 7149–7168. DOI: https://doi.org/10.5194/acp-18-7149-2018

**Kim, YP** and **Lee, G.** 2018. Trend of air quality in Seoul: Policy and science. *Aerosol and Air Quality Res.* **18**: 2141–2156. DOI: https://doi.org/10.4209/aaqr.2018.03.0081

**Korea Meteorological Administration (KMA).** 2009. https://web.kma.go.kr/eng/biz/climate_01.jsp (accessed Jun 2019).

**Korean Ministry of Environment (KMOE).** 2017. http://eng.me.go.kr/eng/web/index.do?menuId=221 (accessed Feb 2019).

**Korea Herald.** 2018. http://www.koreaherald.com/view.php?ud=20181115000516 (accessed Feb 2019).

**Korea LPG Association (KLPG).** 2004. http://www.klpg.or.kr/front/english/lpg/lpg_use.html (accessed May 2019).

**Kovacs, TA, Brune, WH, Harder, H, Martinez, M, Simpas, JB, Frost, GJ, Williams, E, Jobson, T, Stroud, C, Young, V, Fried, A** and **Wert, B.** 2003. Direct measurements of urban OH reactivity during Nashville SOS in summer 1999. *J. Environ. Monit.* **5**: 68–74. DOI: https://doi.org/10.1039/b204339d

**Kwon, K-D, Jo, W-K, Lim, H-J** and **Jeong, WS.** 2007. Characterization of emissions composition for selected household products available in Korea. *J. Hazard. Mat.* **148**: 192–198. DOI: https://doi.org/10.1016/j.jhazmat.2007.02.025

**Lamb, KD, Perring, AE, Samset, B, Peterson, D, Davis, S, Anderson, BE, Beyersdorf, A, Blake, DR, Campuzano-Jost, P, Corr, CA, Diskin, GS, Kondo, Y, Moteki, N, Nault, B, Oh, J, Park, M, Pusede, SE, Simpson, IJ, Thornhill, L, Wisthaler, A** and **Schwarz, J.** 2018. Estimating source region influences on black carbon abundance, microphysics and radiative effect observed over South Korea. *J. Geophys. Res.* **123**: 13,527–13,548. DOI: https://doi.org/10.1029/2018JD029257

**Lee, DG, Lee, Y-M, Jang, K-W, Yoo, C, Kang, K-H, Lee, J-H, Jung, S-W, Park, J-M, Lee, S-B, Han, J-S, Hong, J-H** and **Lee, S-J.** 2011. Korean national emissions inventory system and 2007 air pollutant emissions. *Asian J. Atmos. Environ.* **5**(4): 278–291. DOI: https://doi.org/10.5572/ajae.2011.5.4.278

**Lee, H-J, Jo, H-Y, Kim, S-W, Park, M-S** and **Kim, C-H.** 2019. Impacts of atmospheric vertical structures on transboundary aerosol transport from China to South Korea. *Scientific Reports* **9**: 13040. DOI: https://doi.org/10.1038/s41598-019-49691-z

**Li, M, Zhang, Q, Zheng, B, Tong, D, Lei, Y, Liu, F, Hong, C, Kang, S, Yan, L, Zhang, Y, Bo, Y, Su, H, Cheng, Y** and **He, K.** 2019. Persistent growth of anthropogenic non-methane volatile organic compound (NMVOC) emissions in China during 1990–2017: drivers, speciation and ozone formation potential. *Atmos. Chem. Phys.* **19**: 8897–8913. DOI: https://doi.org/10.5194/acp-19-8897-2019

**Liu, Y, Shao, M, Lu, S, Chang, C-C, Wang, J-L** and **Chen, G.** 2008. Volatile Organic Compound (VOC) measurements in the Pearl River Delta (PRD) region, China. *Atmos. Chem. Phys.* **8**: 1531–1545. www.atmos-chem-phys.net/8/1531/2008. DOI: https://doi.org/10.5194/acp-8-1531-2008

**Lunt, MF, Park, S, Li, S, Henne, S, Manning, AJ, Ganesan, AL, Simpson, IJ, Blake, DR, Liang, Q, O'Doherty, S, Harth, CM, Mühle, J, Salameh, PK,**

**Weiss, RF, Krummel, PB, Fraser, PJ, Prinn, RG, Reimann, S** and **Rigby, M.** 2018. Continued emissions of the ozone-depleting substance carbon tetrachloride from Eastern Asia. *Geophys. Res. Lett.* **45**. DOI: https://doi.org/10.1029/2018GL079500

**Lyu, XP, Zeng, LW, Guo, H, Simpson, IJ, Ling, ZH, Wang, Y, Murray, F, Louie, PKK, Saunders, SM, Lam, SHM** and **Blake, DR.** 2017. Evaluation of the effectiveness of air pollution control measures in Hong Kong. *Environ. Poll.* **220**: 87–94. DOI: https://doi.org/10.1016/j.envpol.2016.09.025

**Ministry of Land, Infrastructure and Transport (MOLIT).** 2016. https://www.ceicdata.com/en/korea/number-of-registered-motor-vehicles-by-fuel-types. Accessed June 2019.

**McDonald, BC, de Gouw, JA, Gilman, JB, Jathar, SH, Akherati, A, Cappa, CD, Jimenez, JL, Lee-Taylor, J, Hayes, PL, McKeen, SA, Cui, YY, Kim, S-W, Gentner, DR, Isaacman-VanWertz, G, Goldstein, AH, Harley, RA, Frost, GJ, Roberts, JM, Ryerson, TB** and **Trainer, M.** 2018. Volatile chemical products emerging as largest petrochemical source of urban organic emissions. *Science* **359**: 760–764. DOI: https://doi.org/10.1126/science.aaq0524

**McGaughey, GR, Desai, NR, Allen, DT, Seila, RL, Lonneman, WA, Fraser, MP, Harley, RA, Pollack, AK, Ivy, JM** and **Price, JH.** 2004. Analysis of motor vehicle emissions in a Houston tunnel during the Texas Air Quality Study 2000. *Atmos. Environ.* **38**: 3363–3372. DOI: https://doi.org/10.1016/j.atmosenv.2004.03.006

**Montzka, SA, Dutton, GS, Yu, P, Ray, E, Portmann, RW, Daniel, JS, Kuijpers, L, Hall, BD, Mondeel, D, Siso, C, Nance, JD, Rigby, M, Manning, AJ, Hu, L, Moore, F, Miller, BR** and **Elkins, JW.** 2018. An unexpected and persistent increase in global emissions of ozone-depleting CFC-11. *Nature* **557**: 413–417. DOI: https://doi.org/10.1038/s41586-018-0106-2

**Müller, M, Mikoviny, T, Feil, S, Haidacher, S, Hanel, G, Hartungen, E, Jordan, A, Märk, L, Mutschlechner, P, Schottkowsky, R, Sulzer, P, Crawford, JH** and **Wisthaler, A.** 2014. A compact PTR-ToF-MS instrument for airborne measurements of volatile organic compounds at high spatiotemporal resolution. *Atmos. Meas. Tech.* **7**: 3763–3772. DOI: https://doi.org/10.5194/amt-7-3763-2014

**Na, K.** 2006. Determination of VOC source signature of vehicle exhaust in a traffic tunnel. *J. Environ. Management* **81**(4): 392–398. DOI: https://doi.org/10.1016/j.jenvman.2005.11.004

**Na, K** and **Kim, YP.** 2001. Seasonal characteristics of ambient volatile organic compounds in Seoul. *Atmos. Environ.* **35**(15): 2603–2614. DOI: https://doi.org/10.1016/S1352-2310(00)00464-7

**Na, K, Kim, YP, Moon, I** and **Moon, K-C.** 2004. Chemical composition of major VOC emission sources in the Seoul atmosphere. *Chemosphere* **55**: 585–594. DOI: https://doi.org/10.1016/j.chemosphere.2004.01.010

**Na, K, Moon, K-C** and **Kim, YP.** 2005. Source contribution to aromatic VOC concentration and ozone formation potential in the atmosphere of Seoul. *Atmos. Environ.* **39**: 5517–5524. DOI: https://doi.org/10.1016/j.atmosenv.2005.06.005

**Nault, BA, Campuzano-Jost, P, Day, DA, Schroder, JC, Anderson, B, Beyersdorf, AJ, Blake, DR, Brune, WH, Choi, Y, Corr, CA, de Gouw, JA, Dibb, J, DiGangi, JP, Diskin, GS, Fried, A, Huey, LG, Kim, MJ, Knote, CJ, Lamb, KD, Lee, T, Park, T, Pusede, SE, Scheuer, E, Thornhill, KL, Woo, J-H** and **Jimenez, JL.** 2018. Secondary organic aerosol production from local emissions dominates the organic aerosol budget over Seoul, South Korea, during KORUS-AQ. *Atmos. Chem. Phys.* **18**: 17,769–17,800. DOI: https://doi.org/10.5194/acp-18-17769-2018

**Nguyen, HT, Kim, K-H** and **Kim, M-Y.** 2009. Volatile organic compounds at an urban monitoring station in Korea. *J. Hazard. Materials* **161**: 163–174. DOI: https://doi.org/10.1016/j.jhazmat.2008.03.066

**Norris, G, Duvall, R, Brown, S** and **Bai, S.** 2014. *EPA Positive Matrix Factorization (PMF) 5.0 Fundamentals and User Guide, EPA/600/R-14/108.* Washington, DC: U.S. Environmental Protection Agency, Office of Research and Development.

**Ou, J, Guo, H, Zheng, J, Cheung, K, Louie, PKK, Ling, Z** and **Wang, D.** 2015. Concentrations and sources of non-methane hydrocarbons (NMHCs) from 2005 to 2013 in Hong Kong: A multi-year real-time analysis. *Atmos. Environ.* **103**: 196–206. DOI: https://doi.org/10.1016/j.atmosenv.2014.12.048

**Paatero, P, Eberly, S, Brown, SG** and **Norris, GA.** 2014. Methods for estimating uncertainty in factor analytic solutions. *Atmos. Meas. Tech.* **7**: 781–797. DOI: https://doi.org/10.5194/amt-7-781-2014

**Pang, Y, Fuentes, M** and **Rieger, P.** 2014. Trends in the emissions of volatile organic compounds (VOCs) from light-duty gasoline vehicles tested on chassis dynamometers in Southern California. *Atmos. Environ.* **83**: 127–135. DOI: https://doi.org/10.1016/j.atmosenv.2013.11.002

**Peterson, DA, Hyer, EJ, Han, S-O, Crawford, JH, Park, RJ, Holz, R, Kuehn, RE, Eloranta, E, Knote, C, Jordan, CE** and **Lefer, BL.** 2019. Meteorology influencing springtime air quality, pollution transport, and visibility in Korea. *Elem Sci Anth.* **7**: 57. DOI: https://doi.org/10.1525/elementa.395

**Richter, D, Weibring, P, Walega, JG, Fried, A, Spuler, SM** and **Taubman, MS.** 2015. Compact highly sensitive multi-species airborne mid-IR spectrometer. *Appl. Phys. B* **119**(1): 119–131. DOI: https://doi.org/10.1007/s00340-015-6038-8

**Rigby, M, Park, S, Saito, T, Western, LM, Redington, AL, Fang, X, Henne, S, Manning, AJ, Prinn, RG, Dutton, GS, Fraser, PJ, Ganesan, AL, Hall, BD, Harth, CM, Kim, J, Kim, KR, Krummel, PB, Lee, T, Li, S** and **Liang, Q.** 2019. Increase in CFC-11 emissions from eastern China based on atmospheric observations. *Nature.* DOI: https://doi.org/10.1038/s41586-019-1193-4

**Russo, RS, Zhou, Y, White, ML, Mao, H, Talbot, R** and **Sive, BC.** 2010. Multi-year (2004–2008) record of nonmethane hydrocarbons in New England: seasonal variations and regional sources. *Atmos. Chem. Phys.* **10**: 4909–4929. DOI: https://doi.org/10.5194/acp-10-4909-2010

**Ryerson, TB, Trainer, M, Angevine, WM, Brock, CA, Dissly, RW, Fehsenfeld, FC, Frost, GJ, Goldan, PD, Holloway, JS, Hübler, G, Jakoubek, RO, Kuster, WC, Neuman, JA, Nicks, DK Jr., Parrish, DD, Roberts, JM, Sueper, DT, Atlas, EL, Donnelly, SG, Flocke, F, Fried, A, Potter, WT, Schauffler, S, Stroud, V, Weinheimer, AJ, Wert, BP, Wiedinmyer, C, Alvarez, RJ, Banta, RM, Darby, LS** and **Senff, CJ.** 2003. Effect of petrochemical industrial emissions of reactive alkenes and $NO_x$ on tropospheric ozone formation in Houston, Texas. *J. Geophys. Res.* **108**(D8): 4249. DOI: https://doi.org/10.1029/2002JD003070

**Schroeder, JS, Crawford, JH, Ahn, J-Y, Chang, L, Fried, A, Walega, J, Weinheimer, A, Montzka, DD, Hall, SR, Ullmann, K, Wisthaler, A, Mikoviny, T, Chen, G, Blake, DR, Blake, NJ, Hughes, SC, Meinardi, S, Diskin, G, Digangi, JP, Choi, Y, Pusede, SE, Huey, GL, Tanner, DJ, Kim, M** and **Wennberg, P.** 2020. Observation-based modeling of ozone chemistry in the Seoul metropolitan area during the Korea-United States Air Quality Study. *Elem. Sci. Anth.* **8**: 3. DOI: https://doi.org/10.1525/elementa.400

**Seo, J, Park, D-S R, Kim, JY, Young, D, Lim, YB** and **Kim, Y.** 2018. Effects of meteorology and emissions on urban air quality: a quantitative statistical approach to long-term records (1999–2016) in Seoul, South Korea. *Atmos. Chem. Phys.* **18**: 16,121–16,137. DOI: https://doi.org/10.5194/acp-18-16121-2018

**Shen, L, Xiang, P, Liang, S, Chen, W, Wang, M, Lu, S** and **Wang, Z.** 2018. Source profiles of volatile organic compounds (VOCs) measured in a typical industrial process in Wuhan, central China. *Atmosphere* **9**: 297. DOI: https://doi.org/10.3390/atmos9080297

**Shin, HJ, Kim, JC, Lee, SJ** and **Kim, YP.** 2013. Evaluation of the optimum volatile organic compounds control strategy considering the formation of ozone and secondary organic aerosol in Seoul, Korea. *Environ. Sci. Pollut. Res.* **20**(3): 1468–1481. DOI: https://doi.org/10.1007/s11356-012-1108-5

**Simpson, IJ, Aburizaiza, OS, Siddique, A, Barletta, B, Blake, NJ, Gartner, A, Khwaja, H, Meinardi, S, Zeb, J** and **Blake, DR.** 2014. Air quality in Mecca and surrounding holy places in Saudi Arabia during Hajj: Initial survey. *Environ. Sci. Technol.* **48**: 8529–8539. DOI: https://doi.org/10.1021/es5017476

**Simpson, IJ, Blake, NJ, Barletta, B, Diskin, GS, Fuelberg, HE, Gorham, K, Huey, LG, Meinardi, S, Rowland, FS, Vay, SA, Weinheimer, AJ, Yang, M** and **Blake, DR.** 2010. Characterization of trace gases measured over Alberta oil sands mining operations: 76 speciated $C_2$–$C_{10}$ volatile organic compounds (VOCs), $CO_2$, $CH_4$, CO, NO, $NO_2$, $NO_y$, $O_3$ and $SO_2$. *Atmos. Chem. Phys.* **10**: 11,931–11,954. DOI: https://doi.org/10.5194/acp-10-11931-2010

**Smith, ML, Kort, EA, Karion, A, Sweeney, C, Herndon, SC** and **Yacovitch, TI.** 2015. Airborne ethane observations in the Barnett Shale: Quantification of ethane flux and attribution of methane emissions. *Environ. Sci. Tech.* **49**: 8158–8166. DOI: https://doi.org/10.1021/acs.est.5b00219

**Song, M, Tan, Q, Feng, M, Qu, Y, Liu, X, An, J** and **Zhang, Y.** 2018. Source apportionment and secondary transformation of atmospheric nonmethane hydrocarobns in Chengdu, Southwest China. *J. Geophys. Res.* **123**: 9741–9763. DOI: https://doi.org/10.1029/2018JD028479

**Spinei, E, Whitehill, A, Fried, A, Tiefengraber, M, Knepp, TN, Herndon, S, Herman, JR, Müller, M, Abuhassan, N, Cede, A, Richter, D, Walega, J, Crawford, J, Szykman, J, Valin, L, Williams, DJ, Long, R, Swap, RJ, Lee, Y, Nowak, N** and **Poche, B.** 2018. The first evaluation of formaldehyde column observations by improved Pandora spectrometers during the KORUS-AQ field study. *Atmos. Meas. Tech.* **11**: 4943–4961. DOI: https://doi.org/10.5194/amt-11-4943-2018

**Stohl, A, Forster, C, Frank, A, Seibert, P** and **Wotawa, G.** 2005. Technical Note: The Lagrangian particle dispersion model FLEXPART version 6.2. *Atmos. Chem. Phys.* **5**: 2461–2474. DOI: https://doi.org/10.5194/acp-5-2461-2005

**Tang, JH, Chu, KW, Chan, LY** and **Chen, YJ.** 2014. Non-methane hydrocarbon emission profiles from printing and electronic industrial processes and its implications on the ambient atmosphere in the Pearl River Delta, South China. *Atmos. Pollut. Res.* **5**: 151–160. DOI: https://doi.org/10.5094/APR.2014.019

**Tang, W, Emmons, LK, Arellano, AF, Jr, Gaubert, B, Knote, C, Tilmes, S, Buchholz, RR, Pfister, GG, Diskin, GS, Blake, DR, Blake, NJ, Meinardi, S, DiGangi, JP, Choi, Y, Woo, JH, He, C, Schroeder, JR, Suh, I, Lee, HJ, Jo, HY, Kanaya, Y, Jung, J, Lee, Y** and **Kim, D.** 2019. Source contributions to carbon monoxide concentrations during KORUS-AQ based on CAM-chem model applications. *J. Geophys. Res.* **124**: 2796–2822. DOI: https://doi.org/10.1029/2018JD029151

**Tilmes, S, Lamarque, J-F, Emmons, LK, Kinnison, DE, Ma, P-L, Liu, X, Ghan, S, Bardeen, C, Arnold, S, Deeter, M, Vitt, F, Ryerson, T, Elkins, JW, Moore, F, Spackman, JR** and **Val Martin, M.** 2015. Description and evaluation of tropospheric chemistry and aerosols in the Community Earth System Model (CESM1.2). *Geosci. Model Dev.* **8**: 1395–1426. DOI: https://doi.org/10.5194/gmd-8-1395-2015

**Tsai, J-H, Chang, S-Y** and **Chiang, H.-L.** 2012. Volatile organic compounds from the exhaust of light-duty diesel vehicles. *Atmos. Environ.* **61**: 499–506. DOI: https://doi.org/10.1016/j.atmosenv.2012.07.078

**Vollmer, MK, Zhou, LX, Greally, BR, Henne, S, Yao, B, Reimann, S, Stordal, F, Cunnold, DM, Zhang, XC, Maione, M, Zhang, F, Huang, J** and **Simmonds, PG.** 2009. Emissions of ozone-depleting halocarbons from China. *Geophys. Res. Lett.* **36**: L15823. DOI: https://doi.org/10.1029/2009GL038659

**Wang, G, Cheng, S, Wei, W, Zhou, Y, Yao, S** and **Zhang, H.** 2016. Characteristics and source apportionment of VOCs in the suburban area of Beijing, China. *Atmos. Pollut. Res.* **7**: 711–724. DOI: https://doi.org/10.1016/j.apr.2016.03.006

**Wang, H, Qiao, Y, Chen, C, Lu, J, Dai, H, Qiao, L** and **Wu, J.** 2014. Source profiles and chemical reactivity of volatile organic compounds from solvent use in Shanghai, China. *Aerosol Air Qual. Res.* **14**(1): 301–310. DOI: https://doi.org/10.4209/aaqr.2013.03.0064

**Wang, H-L, Jing, S-A, Lou, S-R, Hu, Q-Y, Li, L, Tao, S-K, Huang, C, Qiao, L-P** and **Chen, C-H.** 2017. Volatile organic compounds (VOCs) source profiles of on-road vehicle emissions in China. *Sci. Total Environ.* **607–608**: 253–261. DOI: https://doi.org/10.1016/j.scitotenv.2017.07.001

**Wang, Y, Ren, X, Ji, D, Zhang, J, Sun, J** and **Wu, F.** 2016. Characterization of volatile organic compounds in the urban area of Beijing from 2000 to 2007. *J. Environ. Sci.* **24**(1): 95–101. DOI: https://doi.org/10.1016/S1001-0742(11)60732-8

**Warner, J, Wei, Z, Strow, L, Barnet, CD, Sparling, LC, Diskin, GS** and **Sachse, G.** 2010. Improved agreement of AIRS tropospheric carbon monoxide products with other EOS sensors using optimal estimation retrievals. *Atmos. Chem. Phys.* **10**: 9521–9533. DOI: https://doi.org/10.5194/acp-10-9521-2010

**Weinheimer, AJ, Walega, JG, Ridley, BA, Gary, BL, Blake, DR, Blake, NJ, Rowland, FS, Sachse, GW, Anderson, BE** and **Collins, JE.** 1994. Meridional distributions of $NO_x$, $NO_y$, and other species in the lower stratosphere and upper troposphere during AASE II. *Geophys. Res. Lett.* **21**: 2583–2586. DOI: https://doi.org/10.1029/94GL01897

**Woo, J-H, Choi, K-C, Kim, HK, Baek, BH, Jang, M, Eum, J-H, Song, CH, Ma, Y-I, Sunwoo, Y, Chang, L-S** and **Yoo, SH.** 2012. Development of anthropogenic emissions processing system for Asia using SMOKE. *Atmos. Environ.* **58**: 5–13. DOI: https://doi.org/10.1016/j.atmosenv.2011.10.042

**Wu, F, Yu, Y, Sun, J, Zhang, J, Wang, J, Tang, G** and **Wang, Y.** 2016. Characteristics, source apportionment and reactivity of ambient volatile organic compounds at Dinghu Mountain in Guangdong Province, China. *Sci. Total Environ.* **548–549**: 347–359. DOI: https://doi.org/10.1016/j.scitotenv.2015.11.069

**Wu, R** and **Xie, S.** 2017. Spatial distribution of ozone formation in China derived from emissions of speciated volatile organic compounds. *Environ. Sci. Technol.* **51**: 2574–2583. DOI: https://doi.org/10.1021/acs.est.6b03634

**Yao, Z, Shen, X, Ye, Y, Cao, X, Jiang, X, Zhang, Y** and **He, K.** 2015. On-road emission characteristics of VOCs from diesel trucks in Beijing, China. *Atmos. Environ.* **103**: 87–93. DOI: https://doi.org/10.1016/j.atmosenv.2015.01.054

**Yang, Y, Shao, M, Wang, X, Nölscher, AC, Kessel, S, Guenther, A** and **Williams, J.** 2016. Towards a quantitative understanding of total OH reactivity: A review. *Atmos. Environ.* **134**: 147–161. DOI: https://doi.org/10.1016/j.atmosenv.2016.03.010

**Yuan, B, Shao, M, de Gouw, J, Parrish, DD, Lu, S, Wang, M, Zeng, L, Zhang, Q, Song, Y, Zhang, J** and **Hu, M.** 2012. Volatile organic compounds (VOCs) in urban air: How chemistry affects the interpretation of positive matrix factorization (PMF) analysis. *J. Geophys. Res.* **117**: D24302. DOI: https://doi.org/10.1029/2012JD018236

**Yuan, B, Shao, M, Lu, S** and **Wang, B.** 2010. Source profiles of volatile organic compounds associated with solvent use in Beijing, China. *Atmos. Environ.* **44**: 1919–1926. DOI: https://doi.org/10.1016/j.atmosenv.2010.02.014

**Yue, T, Yie, X, Chai, F, Hu, J, Lai, Y, He, L** and **Zhu, R.** 2017. Characteristics of volatile organic compounds (VOCs) from the evaporative emissions of modern passenger cars. *Atmos. Environ.* **151**: 62–69. DOI: https://doi.org/10.1016/j.atmosenv.2016.12.008

**Zheng, J, Yu, Y, Mo, Z, Zhang, Z, Wang, X, Yin, S, Peng, K, Yang, Y, Feng, Z** and **Cai, H.** 2013. Industrial sector-based volatile organic compound (VOC) source profiles measured in manufacturing facilities in the Pearl River Delta, China. *Sci. Total Environ.* **456–457**: 127–136. DOI: https://doi.org/10.1016/j.scitotenv.2013.03.055

**How to cite this article:** Simpson, IJ, Blake, DR, Blake, NJ, Meinardi, S, Barletta, B, Hughes, SC, Fleming, LT, Crawford, JH, Diskin, GS, Emmons, LK, Fried, A, Guo, H, Peterson, DA, Wisthaler, A, Woo, J-H, Barré, J, Gaubert, B, Kim, J, Kim, MJ, Kim, Y, Knote, C, Mikoviny, T, Pusede, SE, Schroeder, JR, Wang, Y, Wennberg, PO and Zeng, L. 2020. Characterization, sources and reactivity of volatile organic compounds (VOCs) in Seoul and surrounding regions during KORUS-AQ. *Elem Sci Anth*, 8: 37. DOI: https://doi.org/10.1525/elementa.434

**Domain Editor-in-Chief:** Detlev Helmig, Institute of Alpine and Arctic Research, University of Colorado Boulder, US

**Associate Editor:** Jochen Stutz, Atmospheric and Oceanic Sciences, University of California Los Angeles, US

**Knowledge Domain:** Atmospheric Science

**Part of an *Elementa* Special Feature:** KORUS-AQ

**Submitted:** 06 December 2019 **Accepted:** 23 June 2020 **Published:** 11 August 2020



ELEMENTA Science of the Anthropocene

*Elem Sci Anth* is a peer-reviewed open access journal published by University of California Press.

OPEN ACCESS